iScience

CellPress
OPEN ACCESS

Review

Improving thermal conductivities of textile materials by nanohybrid approaches

Ozlem Ipek Kalaoglu-Altan,[1] Burcak Karaguzel Kayaoglu,[1] and Levent Trabzon[2,3,4,*]

SUMMARY

The thermal transfer between individual body and the surroundings occurs by several paths such as radiation, evaporation, conduction, and convection. Thermal management is related with the heat transfer between the human body and the surroundings, which aims to keep the body temperature in the comfort range either via preserving or via emitting the body heat. The essential duty of clothing is to contribute to the thermal balance of the human body by regulating the heat and moisture transfer. In the case of poorly controlled body heat, health problems such as hyperthermia and heatstroke along with environmental problems due to higher energy consumption can occur. Recently, research has been focused on advanced textiles with novel approaches on materials synthesis and structure design, which can provide thermal comfort together with energy saving. This review article focuses on the innovative strategies basically on the passive textile models for improved thermal conductivity. We will discuss both the fabrication techniques and the inclusion of carbon-based and boron-based fillers to form nano-hybrid textile solutions, which are used to improve the thermal conductivity of the materials.

INTRODUCTION

Thermal comfort is defined as the condition of human mind satisfied with its thermal environment, in terms of whether they feel too hot or too cold and is affected by metabolic heat produced by the body, clothing, air temperature, radiant heat, humidity, and air movement (Fanger, 1970). Among the functions of a textile clothing, protection against a variety of weather conditions and maintenance of consumers' comfort level via regulating the body surface temperature rank in priority (Akcagun et al., 2019; Zimniewska et al., 2002). It should also assure sufficient heat transfer between human body and outer environment surroundings via providing thermal insulation or reducing heat flow from the body to a colder environment in order to preserve the physiological thermal balance of the wearer. The body of a human being is itself a thermoregulated organism generating H_2O, heat, and other substances due to cellular respiration, muscle functions, and digestion of food. The most comfortable body temperature of a human skin is considered to be 33.4°C, and a deviation about $\pm$4.5°C causes thermal discomfort (Peng et al., 2019; Maughan, 2003). The adaptation to the change in the body heat is mostly provided by skin with symptoms such as horripilation, severe sweating, or nose secretion. Clothing is a key factor in thermal management process because it regulates the heat and moisture transfer between human and environment. Traditional clothing materials can provide limited thermal management, so novel advanced textile materials should be designed and fabricated, which can be adaptive, responsive and also breathable, flexible, and light (Tabor et al., 2020). Conventional textiles are not sufficient in adapting to the changes in the temperature of skin microclimate, which is a tiny air gap between clothing and skin. The thermal comfort of humans largely depends on the temperature and moisture of the microclimate, so thermal management can be improved by fabricating smart textiles that can self-adapt the microclimate temperature in any weather condition (Zou et al., 2021). Several commercialized textiles with improved thermal comfort properties have been developed by various sportswear brands such as Omni-heat (Columbia), CoolMax/Thermolite (Dupont), AeroReact (Nike), Dri-FIT (Nike), HeatGear/ColdGear (Under Armour), Gore-Tex, etc. Omni-heat contains little silver dots, which reflect body heat to keep body warmer. Coolmax and Thermolite use recycled polyester for moisture-wicking property and lightweight insulation, respectively. Bicomponent yarn structure in AeroReact senses moisture vapor and opens its structure to increase breathability. Dri-FIT uses unique polyester-based microfiber construction to provide body cooling via wicking away and dispersing sweat throughout the fabric surface. HeatGear and ColdGear are created with performance fabric that keeps body cool, dry, and light in warm conditions and warm, dry, and light in cold conditions, respectively. Gore-tex is an expanded

[1]Istanbul Technical University, Department of Textile Engineering, Beyoglu, Istanbul 34437, Turkey

[2]Istanbul Technical University, Department of Mechanical Engineering, Beyoglu, Istanbul 34437, Turkey

[3]Istanbul Technical University, MEMS Research Center, Maslak, Istanbul 34469, Turkey

[4]Nanotechnology Research and Application Center – ITUnano, Istanbul Technical University, Maslak, Istanbul 34469, Turkey

*Correspondence: trabzonl@itu.edu.tr

https://doi.org/10.1016/j.isci.2022.103825

polytetrafluoroethylene-based waterproof and breathable fabric widely used in active and sportswear. Directaplus has produced graphene-enhanced co-masks with its patented planar thermal circuit invention, as well as ski jackets and trousers. The thermal conductivity of the material is an important property because it affects the heat flow in the material. Heat flow through the clothing basically depends on the thermal conductivity of the fibrous material, fiber volume content, construction of the fabric, and orientation of fiber with regard to the heat flow direction (Siddiqui and Sun, 2017). Heat can be transferred from clothing to the environment to maintain its thermal balance through conduction, convection, and radiation and evaporation (Peng et al., 2019; Stevens and Fuller, 2015; Hu et al., 2020a; Zhang et al., 2021). The thermal conduction depends on the thermal conductivity, fibrous morphology, and size, whereas air permeability and moisture absorption come along with porosity, wettability, and surface area of the fabric. In hot weather, the fast evaporation of the sweat from the fabric is favorable, whereas in winter clothing low breathability is preferential to maintain the body temperature at the comfort level. Heat conduction is an effective factor for human body heat dissipation either to raise or to decrease human body heat loss for personal thermal management along with being the only route of heat dissipation throughout the textile itself. Especially for IR-opaque textiles, heat conduction surpasses radiation in heat transport mechanism. Hence, heat conductive textiles are attractive for personal thermoregulation to adjust the body temperature (Peng and Cui, 2020).

The general heat balance equation for the heat exchange between an individual and environment can be described as (Song et al., 2011):

$$S = M - W - E - R - C - K$$

where S is the heat stored in the body, M is the metabolic heat generated by the body cells through biochemical reactions, W is the total external work performed by the body, E is the evaporative heat flow as heat dissipates from body when sweat evaporates, R is the radiative heat flow between human body and surrounding hot or cold objects, K is the conductive heat flow between a human body and surrounding objects through direct contact, and C is the heat exchange through clothing. When the human body is in thermal comfort, S should be zero. When S is positive, the body temperature rises, leading to the vasodilation of blood and sweating. If S is negative, heat is radiated from the body to the surroundings, causing a decrease in body temperature and eventually to vasoconstriction of the blood vessels and shivering. A thermal balance between the human body and the environment should be set in order to provide thermal comfort to individuals, which is in relation with the heat produced and lost by the body (Song et al., 2011; Oğulata, 2007; Shu et al., 2022). The thermal balance includes heat and moisture exchange between body, clothing, and environment (Djongyang et al., 2010). Thermal conductivity is among important thermal properties of a fabric, which is also related to the breathability of the fabric. A fabric with a high thermal conductivity permits transfer of heat from a hot side, such as the human body to a cooler side such as the air on the other side of clothing. Thermal conductivities of textile structures in general vary from 0.033 to 0.10 W m^{-1} K^{-1} (Akcagun et al., 2019). Reports have given the thermal conductivities of knitted hemp, viscose, linen, cotton, and bamboo fabrics around 0.022 W m^{-1} K^{-1}, 0.031 W m^{-1} K^{-1}, 0.043 W m^{-1} K^{-1}, 0.026–0.065 W m^{-1} K^{-1}, and 0.039–0.045 W m^{-1} K^{-1}, respectively (Stanković et al., 2008; Majumdar et al., 2010; Oner, 2019). The axial thermal conductivity values of silkworm silk fiber ranged between 0.54–6.53 W m^{-1} K^{-1}, whereas the thermal conductivity for wool fabric was reported as 0.043–0.046 W m^{-1} K^{-1} in dry state (Akcagun et al., 2019; Xue et al., 2019). Similarly, polymeric materials also have low thermal conductivities around 0.1–0.5 W m^{-1} K^{-1} (Huang et al., 2018; Zhao and Hu, 2021). The thermal conductivity of both polymeric and conventional textile materials can be improved by the introduction of conductive fillers.

In this article, we will review the recent advances in the enhancement of thermal conductivities of both natural and polymeric materials for thermal regulation properties. Improving the thermal conductivity in terms of fabrication technique and addition of conductive fillers will be discussed. Passive thermoregulation based on thermally advanced materials that can organize the heat generated and dissipated by the human body without use of external energy has been reviewed. Such kind of thermally regulated materials can be obtained via advanced material and fabrication development and design. We will review the contributions of different fabrication techniques such as electrospinning, vacuum filtration, spraying, coating, 3D printing, and chemical coupling, along with different conductive fillers such as carbon-based and boron-based materials on the thermal conductivity, which are summarized in Table 1. Consequently, a brief summary and future perspectives in this field will be given.

Table 1. Thermal conductivities of various materials with different fabrication techniques and filler types

Material	Fabrication Technique	Filler Type	Thermal Conductivity ($Wm^{-1} K^{-1}$)	Remarks	References
Nylon-11	Electrospinning	–	1.6	Hot-spun	(Zhong et al., 2014)
Crystalline polyethylene	Electrospinning	–	9.3		(Ma et al., 2015)
Polyethylene oxide	Electrospinning	–	13–29		(Lu et al., 2017)
Polyvinyl alcohol	Electrospinning		1.23		(Park et al., 2019)
Polystyrene	Electrospinning	GNP	5.0	10 wt % GNP	(Li et al., 2016a)
Polystyrene	Electrospinning followed by hot-press	Thermal rGO	0.689	15 wt % thermal rGO	(Ruan et al., 2018)
Polyamide	Electrospinning	Ag/rGO	2.12	15 wt % Ag/rGO (1/4, w/w)	(Guo et al., 2019a)
Polybenzimidazole	Electrospinning	MWCNT	3.1		(Datsyuk et al., 2020)
Polyvinyl alcohol	Electrospinning and vacuum filtration	BNNS	1.94 (through-plane)	PDMS/PVA/BNNS 15.6 vol % BNNS	(Chen et al., 2017)
Polyimide	Electrospinning	BNNS	13.1	20 wt % BNNS	(Wang et al., 2018a)
Polyvinylidene fluoride	Electrospinning	BN	7.29	30 wt % m-BN	(Zhang et al., 2018)
Polyvinylidene fluoride	Electrospinning	BNNS	10.4 16.3	Thickness of 28 μm Thickness of 18 μm 33 wt % BNNS	(Chen et al., 2019a)
Polyurethane/fluorinated polyurethane	Electrospinning	BNNS	17.9 (in-plane) 0.29 (cross-plane)	18 wt % BNNS	(Yu et al., 2020)
Polyurethane	Electrospinning	BNNS	1.137 (in-plane) 0.182(cross-plane)	60 wt % BNNS	(Miao et al., 2021)
Cellulose nanofiber	Vacuum-assisted filtration	Graphene	164.7	50 wt % graphene	(Chen et al., 2018)
Cellulose nanofiber	Vacuum-assisted filtration	Graphene	7.81	10 wt % TA@PG-CNF	(Wang et al., 2018b)
Nanofibrillated cellulose	Vacuum-assisted filtration	Graphene sheets	14.35	10 wt % ND/G	(Cui et al., 2020)
Cellulose nanofiber	Vacuum-assisted filtration	Ag-rGO	27.55	9.6 wt % Ag-rGO	(Yang et al., 2020)
Cellulose nanofiber	Vacuum-assisted filtration	BNNT	21.39 (in-plane) 4.71 (cross-plane)	25 wt % BNNT 40 wt % BNNT	(Zeng et al., 2017)
Cellulose nanofiber	Vacuum-assisted filtration	BNNT (amine-functional)	12.79 30.25	Thickness of ~90 μm Thickness of ~30 μm 70 wt % BNNT	(Wu et al., 2017)
Cellulose nanofiber	Vacuum-assisted filtration	BNNT (edged hydroxylated)	24.27	60 wt % BNNT	(Wu et al., 2018)
Cellulose nanofiber	Vacuum-assisted filtration	Ag-BNNT	20.9	25 wt % BNNT and 0.199 wt % Ag	(Fu et al., 2018)
Polystyrene	Vacuum-assisted filtration	BNNS-OH	1.131	12 wt % BN-OH	(Han et al., 2020)
Ethylene vinylacetate	Vacuum-assisted filtration	BNNS	13.2	50 wt % BNNS	(Wang et al., 2020)
Cotton	Dipping-drying coating	MWCNT	0.045	Oxygen-containing MWCNT	(Rahman and Mieno, 2015)

(*Continued on next page*)

Table 1. *Continued*

Material	Fabrication Technique	Filler Type	Thermal Conductivity ($Wm^{-1} K^{-1}$)	Remarks	References
Cotton	Dip-pad-cure	Graphene, MWCNT, BN	0.29 ± 0.015 (G) 0.074 ± 0.007 (BN) 0.072 ± 0.007 (MWCNT)	50 wt % 11.1 wt % 11.1 wt %	(Abbas et al., 2013)
Polyamide fabric	Electrophoretic deposition	Graphene oxide nanosheets	0.521		(Zhao et al., 2018a)
Polyester	Knife-over-roll	Graphene nanopowder GNP	0.4243 0.492	200 g/kg graphene 150 g/kg, 0.5 mm thickness	(Manasoglu et al., 2019) (Manasoglu et al., 2021)
Bamboo viscose	Dip-coating	Graphene/CNC	0.136	4 wt % CN, 3 wt % GNP	(Yang et al., 2019)
70% polyester-30% cotton fabric	Dip-coating	MWCNT and graphene	0.704	Coating prepared by casting MWCNT, graphene and WPU	(Dai et al., 2021)
Polyester	Coating	Polyaniline/graphene	0.1843	Graphene/polyaniline = 15%	(Liu and Zhao, 2021)
Merino wool/nylon	Dipping-drying	PEG/PEDOT:PSS/rGO	0.81		(Ghosh et al., 2020)
Polyurethane	Blade coating	GNP	6.28	10 wt % GNP	(Bonetti et al., 2021)
Polyurethane	Blade coating	GNP and BN	6.86	20 wt % GNP, 20 wt % BN	(Soong and Chiu, 2021)
Polyurethane	Doctor blading	GNR and BNNS	0.928	35 wt % BNNS, 50 μgcm^{-2} GNR	(Tan et al., 2020)
Cellulose nanofiber	Doctor blading	BNNS	24.66	50 wt % BNNS	(Chen et al., 2019b)
Cotton	Spraying	MWCNT fluid	0.213		(Yu et al., 2019)
Carbon fabric	Spraying	GNP/epoxy	0.84	0.5 wt % GNP	(Wang and Cai, 2019)
Polyvinyl alcohol nanofiber	Spraying	BNNS	21.4	33.1 wt % BNNS	(Chen et al., 2019c)
Polyurethane	Wet spinning	BNNP	0.262	5 wt % BNNP	(Farajikhah et al., 2019)
Regenerated cellulose	Wet spinning	BNNS	1.682 2.914	60 wt % BNNS Increased draw ratio	(Wu et al., 2019)
Polyvinyl alcohol	3D printing	BNNS	0.078		(Gao et al., 2017)
Polylactic acid	FDM	Nano-graphite	0.32		(Guo et al., 2019b)
Cotton (thiol modified)	Chemical coupling	rGO (thiol modified) WPU (dien modified)	2.13		(Wang et al., 2019)
Polyacrylic acid/polyvinyl alcohol nanofibrous	Chemical coupling	BNNT (amine functional)	0.65		(Kim et al., 2018)
Cellulose fiber	Hot-press	Graphene	9.0	6 wt % of graphene	(Song et al., 2017)
Regenerated cellulose	Solution casting	GNP	5.5 (cross-plane) 800 (in-plane)	25 wt % GNP	(Zahid et al., 2018)
CNT microfibers	Floating catalyst chemical vapor deposition		770		(Gspann et al., 2017)

(*Continued on next page*)

Table 1. *Continued*

Material	Fabrication Technique	Filler Type	Thermal Conductivity (Wm^{-1} K^{-1})	Remarks	References
Ultrahigh molecular weight polyethylene			28.4 ± 3 16 9.5 ± 0.6	Single microfiber Yarn Woven fabric	(Candadai et al., 2020)
Graphene fiber fabric	Spinning, drying, wet-fusing assembly, annealing		301.5		(Li et al., 2016b)
Poly(3-hydroxybutyrate-co-3-hydroxyvalerate)	Compression molding and hot-pressing	h-BN, graphene tube aluminium nitride, aluminium oxide	0.4985 (h-BN/GT) 0.5215 (AN/GT) 0.3534 (h-BN/AO)		(Vishnu Chandar et al., 2021)
Nanofibrillated cellulose-PEG	Evaporation-induced self-Assembly process	Graphene sheets	21.83 (bilayer) 19.37 (5-layer)	30 wt % graphene 20 wt % graphene	(Cui et al., 2019) (Song et al., 2021)
Polypropylene/viscose nonwoven fabric	Nano-soldering	rGO/CNT	2.90		(Tang et al., 2020)
Polyimide	*In situ* polymerization followed by casting	BN/GO	11.203	1 wt % GO and 20 wt % BN	(He and Wang, 2020)

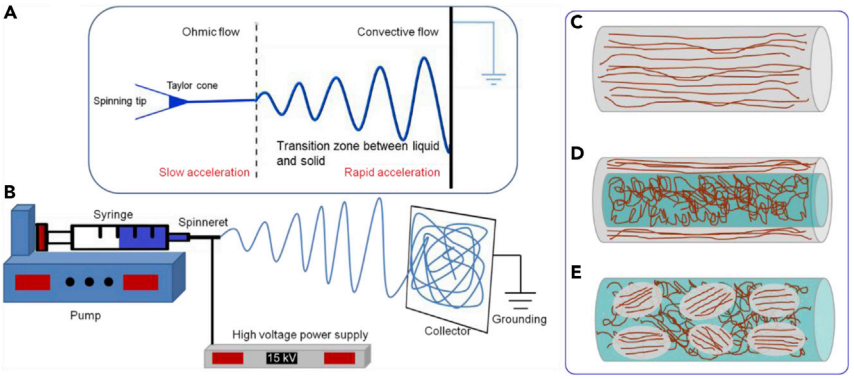

Figure 1. Schematic illustrations for electrospinning technique

(A) Formation of Taylor cone.

(B) Basic electrospinning set-up.

Possible molecular orientations of polymer chains: (C) preferred oriented aligned chains, (D) a core-shell morphology with oriented chains in the outer surface and random chains in the core, (E) a super-molecular morphology with aligned chain spots spread in a randomly oriented chain matrix. Adapted from Canetta et al. (Canetta et al., 2014) with permission from AIP Publishing.

TECHNIQUES USED FOR IMPROVING THERMAL CONDUCTIVITY

Electrospinning

Bulk polymers in general possess low thermal conductivities around 0.1–0.5 W m^{-1} K^{-1} due to their disordered structure (Huang et al., 2018; Chen et al., 2016). A typical polymer structure is composed of both crystalline domains where the chains are regularly oriented and amorphous domains with randomly twisted and entangled chains. In polymers, heat conduction can only be supplied by phonon transfer; however, discontinuous internal interfaces and defects due to the low crystallinity of the polymers cause phonon scattering and decrease phonon transfer efficiency. The crystalline materials tend to show higher thermal conductivity as a result of the ordered structure, and the increase in the polymer chain alignment improves the thermal conductivity by helping the phonon transfer. Researchers have focused to align the polymer chains by several methods including mechanical stretching, nanoscale templating, and electrospinning. Although mechanical stretching and nanoscale templating can also increase the thermal conductivity of polymers significantly, mechanical stretching can cause ruptures in the fibers, which can cause phonon scattering, and heat stretching can lower the crystallinity (Huang et al., 2018). Nanoscale templating is a multistep technique with the need of templating agents and templates.

Electrospinning is a widely used method for the production of nanofibers based on the use of electrostatic forces to draw charged filaments (Bhardwaj and Kundu, 2010; Greiner and Wendorff, 2007). In this technique, a polymer solution or melt is taken in a syringe with a needle, which is placed in a pump to be fed at a constant feed rate (Figure 1). An electrostatic force is applied to the droplet at the tip of the syringe and when the applied tension beats the surface tension, a jet is ejected from the tip to the grounded collector. The solvent evaporates throughout the distance to the collector, leading to fibers with nano-scale diameters. The main factors affecting the chain morphology during electrospinning can be given as the applied voltage and jet speed. It is found out that strengthening the electric field tends to improve the polymer chain alignment, preferably along the axis of the fiber. The jet speed is another important parameter for the alignment. It is a simple and low-cost method, with the advantage of being suitable to a broad diversity of polymer types. However, the process depends on many variables, and thermal conductivity of the as-spun fibers may differ due to the whipping instability (Wei et al., 2021). Moreover, the solvents used in solvent electrospinning can be toxic, and scale-up production may not be feasible.

In a study by Zhong and coworkers, the effect of the size and anisotropic alignment of electrospun aligned Nylon-11 nanofibers on thermal transport was analyzed using high-resolution *in situ* wide-angle X-ray scattering (Zhong et al., 2014). It was revealed the Nylon-11 nanofibers possessed the γ-form among its polymorphs and were stable during electrospinning and hot-stretching. The thermal conductivity of the Nylon-11 nanofibers was increased more than 6 times compared with bulk case with contribution of decreasing fiber diameter and additional axial hot-stretching in improved orientation, crystal size, and

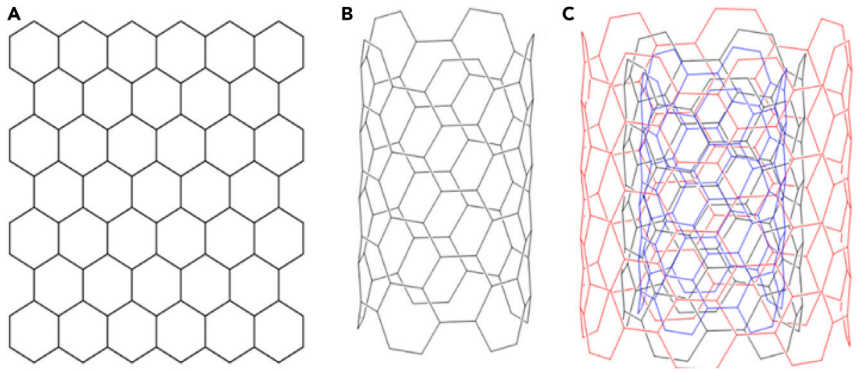

Figure 2. Examples of carbon-based nanofillers
Schematic illustrations of (A) graphene, (B) single-walled carbon nanotube (SWCNT), (C) multi-walled carbon nanotube (MWCNT).

phonon transfer. Ma and coworkers investigated the relation between the structure and thermal conductivity of crystalline PE nanofibers that were electrospun under a voltage between 9–52 kV (Ma et al., 2015). They reached to a maximum value of 9.3 W m^{-1} K^{-1}, which is over 20 times higher compared with the bulk PE under 45 kV at 270 K, suggesting that the PE chains became more oriented under strong elongational force. It was also noted that orthorhombic crystallinity of the chains increased with increasing voltage. The improvement in the thermal conductivity of a semicrystalline polyethylene oxide (PEO) polymers using electrospinning was studied by Lu and coworkers with values between 13–29 W m^{-1} K^{-1} depending on the concentration at a constant relative humidity of 20% (Lu et al., 2017). PEO nanofibers with a crystallinity around 54% preferred a cystalline orientation of [001] lattice direction with a tendency of increasing the thermal conductivity with increased chain alignment in the amorphous region. The electrospinning of PEO increased the thermal conductivity up to 150 times compared with the bulk polymer, proving that this method can also enhance the thermal conductivity of semicrystalline polymers. Seol and coworkers studied the effect of electrospinning polyvinyl alcohol (PVA) and polyvinyl alcohol/cellulose nanocrystal (PVA/CNC) on thermal conductivity and stability (Park et al., 2019). The thermal conductivities of PVA nanofibers and PVA/CNC nanofibers with an average diameter of 200 nm were measured by suspended microdevice technique, respectively, as 1.23 and 0.74 W $m^{-1\ K-1}$ at room temperature, which were higher than that of bulk PVA by factors of 2.5 and 3. The enhancement was due to the increased crystallinity, chain orientation, and also hydrogen bonding for PVA/CNC.

Electrospinning with carbon-based nanofillers

Polymer composites filled with carbon nanomaterials such as graphene, graphene nanoplatelets (GNPs), multiwalled carbon nanotubes (MWCNTs), and single-walled carbon nanotubes (SWCNTs) are regarded as an efficient way for preparing new nanocomposite materials with improved electrical, thermal, and mechanical properties. Two-dimensional planar graphene is a single-layer carbon lattice with a specific hexagonal structure (Figure 2A) (Bitounis et al., 2013). It possesses extraordinary high thermal conductivity around 2000–5300 W m^{-1} K^{-1} in the in-plane direction at room temperature due to the highly ordered structure and stiff sp^2-hybridized bondings, as well as excellent electrical and mechanical properties. Lately, coating various substrates with graphene via methods such as chemical vapor deposition, dip coating, spin coating, spray coating, and electrophoretic deposition has been intensively studied by many research groups (Nooralian et al., 2016; Cui et al., 2020; Chen et al., 2018). Carbon nanotubes are tubular forms of graphene sheets rolled into a cylindrical form with a thermal conductivity around 6600 W m^{-1} K^{-1} in the axial direction, which can be produced at various lengths via mostly arc discharge, laser ablation, or chemical vapor deposition (Gspann et al., 2017). SWCNT consists of a single graphene sheet rolled up into a cylindrical shape, whereas MWCNT comprises several interbedded graphene cylinders (Figures 2B and 2C). CNTs possess high Young's modulus values, thermal stability, and electrical conductivity, making them suitable for reinforced polymer composites (Zhang et al., 2019). However, CNTs are expensive materials, so graphite nanoplatelets (GNPs) with similar properties are found to be a good alternative to CNTs at lower prices. They are usually obtained via "chemical intercalation–hot expansion–ultrasonication" (Gao et al., 2013). GNPs possess a unique layered structure with high aspect ratio and nanoscale thickness. The orientation of the carbon-based nanofillers in the polymer matrix is crucial

in order to transfer the unique properties of the fillers. Hence alignment is particularly preferential to further improve the electrical, thermal, and mechanical properties of the composites with methods such as wet spinning, melt fiber spinning, and electrospinning (Datsyuk et al., 2020).

Polystyrene-graphene nanoplatelet (PS-GNP) nanofibers were prepared by Peijs and coworkers via electrospinning of dimethyformamide (DMF)-stabilized GNP and PS solutions (Li et al., 2016a). The thermal conductivity of PS-GNP nanofibers substantially increased up to nearly 5 W m^{-1} K^{-1} with the addition of 10 wt % GNP, which corresponds to a 630% increase, as well as improved electrical conductivity. In a study by Gu and coworkers, thermal reduced GO (TRGO) was fabricated and TRGO/polystyrene (TRGO/PS) composite fibers were prepared by solution blending and electrospinning, followed by hot-pressing (Ruan et al., 2018). The thermal conductivity and thermal diffusion coefficients of the resulting TRGO/PS composite fibers with 15 wt% TRGO were measured as 0.689 W m^{-1} K^{-1} and 0.6545 mm^2 s^{-1}, which were around 3 times more than that of the pure PS matrix. Both the thermal conductivity and thermal stability of the composites increased with increasing TRGO amount. Guo and coworkers introduced silver nanoparticles anchored reduced graphene oxide (Ag/rGO) fillers with a "point-plane" structure, which were synthesized using one-pot simultaneous reduction of Ag^+ and GO solution via glucose (Guo et al., 2019a). *In situ* polymerized Ag/rGO/polyamide suspension was electrospun and thermally imidized to reveal Ag/rGO/polyimide composite nanofibers. The thermal conductivity of the resulting nanofibers increased to 2.12 W m^{-1} K^{-1} in the presence of 15 wt% Ag/rGO (1/4, w/w), which is about 8 times higher than pure PI. In a study by Datsyuk et al., various carbon nanomaterials such as MWCNTs, SWCNTs, carbon black, GNPs, and graphite were used to produce composite electrospun nanofibers using polybenzimidazole (PBI) polymer with diameters around 120–170 nm (Datsyuk et al., 2020). The maximum thermal conductivity achieved was 3.1 W m^{-1} K^{-1} for MWCNT-PBI nanofibers, indicating an increase of about ~650% compared with neat PBI polymer because MWCNTs were aligned by the fiber axis.

Electrospinning with boron-based nanofillers

Boron nitride (BN), an isoelectronic with carbon, is another thermal conductive material that exists in two crystalline forms, cubical and hexagonal (Abbas et al., 2013). Cubic boron nitride (c-BN) is hard and abrasive with a diamond-like structure, whereas hexagonal boron nitride (h-BN) is smooth and slippery with a white layered crystal structure similar to graphite having a high in-plane thermal conductivity around 300–600 W/mK, which is about 20–30 times that of the thickness direction. Hexagonal boron nitride nanosheets (BNNSs) and boron nitride nanotubes (BNNTs) are analogues to graphene and carbon nanotubes, respectively, but electrically insulating. They have localized electrons due to the ionic characteristic of B−N bonds, wide band gap as well as high phonon velocity that bring in low dielectric constant, high electrical insulation and high thermal conductivity, thermal stability, and elastic modulus (Zeng et al., 2017). Due to the outstanding anisotropy of BN in thermal conductivity, thermal conductivity can be improved in the orientation direction with increased orientation.

Huang and coworkers reported the fabrication of flexible PVA/BNNS/polydimethylsiloxane (PDMS) composites with improved through-plane thermal conductivity for advanced thermal management applications (Chen et al., 2017). PVA/BNNS composite fibers were electrospun and rolled to form a vertically oriented PVA/BNNS cylinder, which were impregnated by PDMS under vacuum to form PDMS/PVA/BNNS nanocomposites. The thermal conductivity of the PDMS/PVA/BNNS nanocomposites with 15.6 vol % BNNS had a through-plane thermal conductivity of 1.94 W m^{-1} K^{-1}, which is 978% higher than pure PDMS. The equilibrium temperature of the LED chip integrated with PDMS/PVA/BNNS nanocomposites was measured about 33°C lower than that of neat PDMS, exposing their potential as thermal interface materials (TIMs). A high temperature thermal conductive, light and flexible nanocomposite textile composed of amino functional boron nitride nanosheets (FBNNS) and polyimide (PI) nanofibers was introduced by Lei and coworkers by green electrospinning of FBNNS and polyamic acid, followed by thermal crosslinking (Wang et al., 2018a). The thermal conductivity of the FBNNS-PI nanofibers was measured as 13.1 W m^{-1} K^{-1} at 300ºC with 20 wt % FBNNS loading, which corresponds to 4,773% increase in comparison with pure PI mat, due to the uniformly dispersed FBNNS in the polymer matrix with vertically aligned orientation. The FBNNS-PI nanofiber mat also exhibited a cooling effect at high temperature, which makes them promising materials for high temperature thermal regulated clothing applications. In a study by Zhang et al., composites with advanced thermal and mechanical properties were prepared using electrospun polyvinylidene fluoride (PVDF) nanofibers and polydopamine (PDA)-modified boron nitride (m-BN) (Zhang et al., 2018). The thermal conductivity of the 30 wt % m-BN loaded composites increased

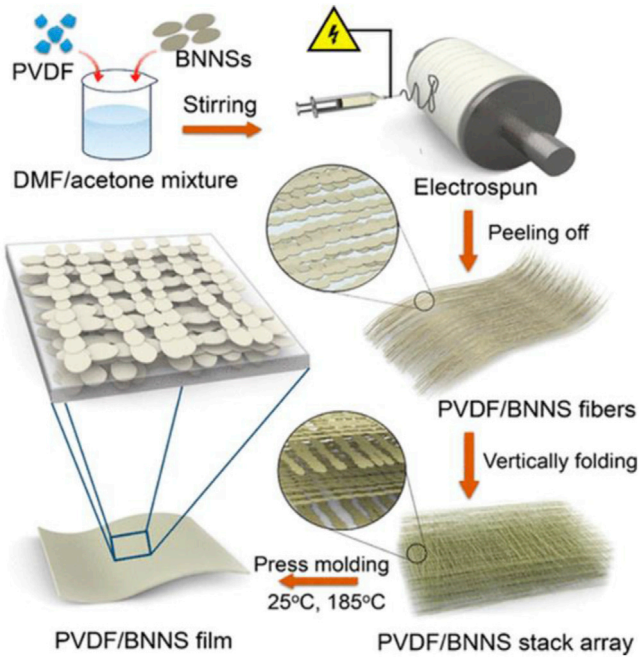

Figure 3. Schematic illustration for the production of the PVDF/BNNS nanocomposite films
Adapted from Chen et al. (Chen et al., 2019a) with permission from ACS Publishing Group.

until 7.29 W m^{-1} K^{-1}, which is 98% higher than that of casting film and 21% higher than electrospun film with BN, due to the strong hydrogen bondings formed as a result of PDA modification and high orientation of m-BN. In addition, tensile strength and Young modulus for the 30 wt % m-BN loaded composites were also improved compared with pure PVDF electrospun films. These flexible composite fibrous films can be potentially used in some flexible electronic applications. A different strategy was adopted by Huang and his group to produce thermally conductive and electrically insulating PVDF/BNNS composites based on electrospinning of a solution containing PVDF and BNNS, folding, and hot-pressing as shown in Figure 3 (Chen et al., 2019a). The 33 wt % BNNS-containing composite film morphologically had an ordered structure and showed an in-plane thermal conductivity of 10.4 W m^{-1} $^{K-1}$ at a thickness of 28 μm, which is 4 times higher than randomly distributed BNNS composites and 2 times higher than directly hot-pressed composites under the same conditions. The thermal conductivity could be increased up to 16.3 W m^{-1} K^{-1} when the thickness decreased to 18 μm. These films also show electrically insulating properties and proved to have a cooling capability, which pave the way to thermal management applications for them.

Ding and coworkers introduced highly thermoconductive and hydrophobic polyurethane (PU)/BNNS composite nanofibers in order to construct thermal management of textiles for personal cooling via electrospinning blends of fluorinated PU, PU, and BNNS, which were linearly oriented along nanofibers (Yu et al., 2020). The maximum in-plane and cross-plane thermal conductivities, respectively, reached to 17.9 W m^{-1} K^{-1} and 0.29 W m^{-1} K^{-1} with FPU/BNNS nanofibers with 18% BNNS electrospun at an RH of 50%. These membranes had a high water vapor transmission rate of 11.6 kg m^{-2} day^{-1}, air permeability of 120 mm s^{-1}, and a high peak heat flux of 0.38 W cm^{-2}. In a recent study by the same group, the hierarchical and interconnected network of vascular plants was adapted to PU/BNNS nanofibrous membranes in order to design multifunctional drying and cooling textiles that allow directional water transport and unblocked heat dissipation throughout perspiration (Figure 4) (Miao et al., 2021). Four layers of membranes were prepared by layer-by-layer assembly of the electrospun aligned PU/BNNS nanofibers with decreasing fiber diameter and capillary pores from inner to outer layers. Sixty wt % BNNS loading in the multilayer nanocomposite resulted in both good mechanical properties with high through-plane and in-plane thermal conductivities of 0.182 W m^{-1} K^{-1} and 1.137 W m^{-1} K^{-1}, respectively. Together with these remarkable thermal conductivities, water transport index of 1,072% and evaporation rate of 0.36 g h^{-1} highlight the capability of these biomimetic textiles for personal drying and cooling.

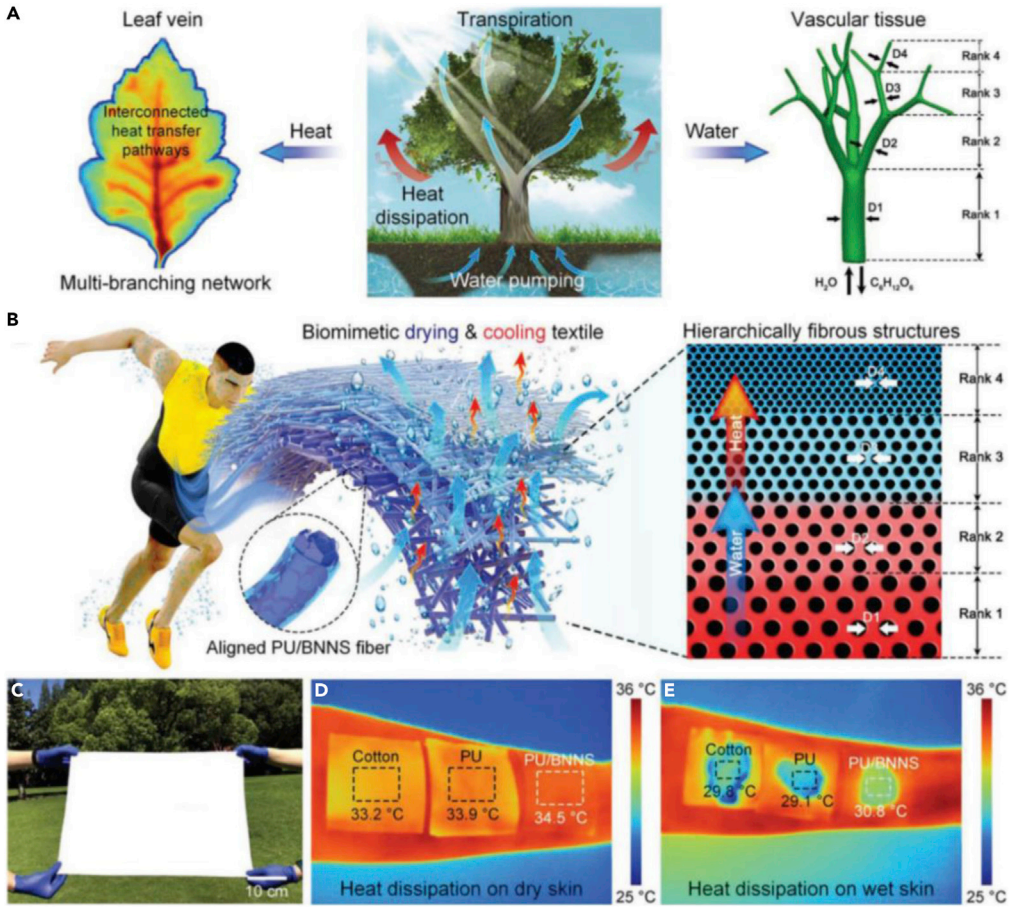

Figure 4. Multifunctional drying and cooling textiles inspired by the transpiration in vascular plants

Schematic illustration of the (A) transpiration in plants, (B) sweat and heat distribution throughout the layer-by-layer structure of the functional textile, (C) photograph of the biomimetic multilayer fibrous membrane. Infrared thermal images of the heat dissipation efficacy of the cotton fabrics, PU multilayers, and PU/BNNS multilayers, (D) under dry and (E) wet conditions. Adapted from Miao et al. (Miao et al., 2021) with permission from Wiley Publishing Group.

Vacuum-assisted filtration

Vacuum-assisted filtration is a frequently used simple technique to produce thermally conductive films using two-dimensional nanofillers with high in-plane thermal conductivity. Although it is possible to fabricate oriented films with high thermal conductivity, this method suffers from low efficiency and long filtration time for good orientation, which can become tougher at higher filler content. This method is also not suitable for scale-up production (Chen et al., 2019b).

Vacuum-assisted filtration of carbon-based nanofillers

Jiang Yu and coworkers prepared flexible cellulose nanofiber/graphene (CNFG) composite films with high thermal conductivity via simple vacuum-assisted filtration (Chen et al., 2018). Five different composites were prepared using 10–50 wt % of 10-μm-sized graphene nanosheets, which were uniformly distributed on the cellulose matrix parallel to the radial direction. In-plane thermal conductivity of 50 wt % graphene-containing composite film (CNFG50) was measured as 164.7 W m^{-1} K^{-1}, which is 253 times higher than neat CNF, whereas the through-plane conductivity was also improved 6 times. Both CNF and CNFG50 preserved their in-plane thermal conductivities for 10 multiple heating and cooling cycles between 25ºC and 100ºC in addition to 1,000 bending cycles. The tensile strength and modulus of CNFG50 were 2 times higher than CNF, which is found to be an excellent heat spreader and dissipater. Hybrid nanostructures were manufactured via *in situ* polymerization of tannic acid and pyrrole on graphene nanosheet containing cellulose nanofibers (TA@PG-CNF) by Huang and coworkers, along with TA@PG-CNF/PVA film fabricated

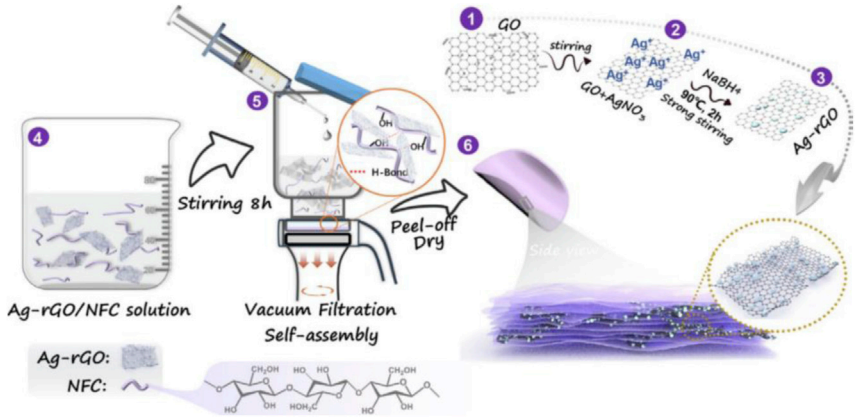

Figure 5. Schematic illustration of the preparation of Ag-rGO and Ag-rGO/NFC hybrid film
Adapted from Yang et al. (Yang et al., 2020) with permission from Elsevier Publishing Group.

under a vacuum-assisted process (Wang et al., 2018b). The conductive pyrrole moiety as well as the strong interactions in the nanohybrid coating and orientation of graphene nanosheets caused improvements in electrical, thermal, and mechanical properties. The thermal and electrical conductivities of the TA@PG-CNF/PVA film reached respectively to 7.81 W m^{-1} K^{-1} and 6.52 S cm^{-1} with 10 wt % filling, in addition to the high tensile strength of 217.9 MPa and toughness of 19.6 MJ m^{-3}. Such nacre-mimetic polymeric materials are influential for the design of portable electronic devices. In a recent study by Ding and colleagues, a composite filler was fabricated using graphene sheets, nano diamond, and 1-pyrenemethylamine hydrochloride (ND/G) to improve the interface between the composite filler and nanofibrillated cellulose (NFC) by vacuum-filtration method, which contributed to the alignment in the system along with the intermolecular hydrogen bonding between fillers and matrix NFC (Cui et al., 2020). The in-plane thermal conductivity of NFC hybrid films modified 10 wt % of the composite filler with ND/G weight ratio of 3:7 was measured as 14.35 W m^{-1} K^{-1}, corresponding to 1,179% increase compared with pure NFC film. These hybrid films were highly flexible with excellent mechanical properties, which also makes them promising for portable electronic devices.

Xie and coworkers fabricated Ag-rGO by a one-pot synchronous reducing method and presented Ag-rGO-functionalized NFC (Ag-rGO/NFC) via vacuum-assisted layer-by-layer assembly (Figure 5) (Yang et al., 2020). An addition of 9.6 wt % Ag-rGO nanosheets resulted in an increase of 1,095% in the in-plane thermal conductivity compared with pure NFC, reaching a value of 27.55 W m^{-1} K^{-1}, as well as an increase of around 573% in the through-plane conductivity attributed to the dense layers of Ag-rGO networks, high static adsorption between GO and Ag+, and hydrogen bonding between GO and NFC. The heat transport rate was also increased from 0.16°C/s to 0.18°C/s with the introduction of Ag-rGO, rising to a surface temperature of 62°C in 220 s. This method is advantageous with low production cost, effective functionalization and industrial feasibility, which encourages the production of multifunctional and lightweight TIMs.

Vacuum-assisted filtration of boron-based nanofillers

Xu and his colleagues constructed a series of cellulose nanofiber and BNNTs composites (CNF-BNNT) with BNNT loading of 0–40 wt % using a combination of ultrasonicated dispersion and vacuum filtration (Zeng et al., 2017). There was an increasing network with overlaps up to 25 wt % BNNT loading that corresponded to an in-plane thermal conductivity of 21.39 W m^{-1} K^{-1}, whereas the out-of-plane thermal conductivity for the nanocomposites continued to increase up to 40 wt % BNNT loading and reached 4.71 W m^{-1} K^{-1}. These nanocomposites also showed a cooling effect and can be attractive for "green" thermal interface materials, printed circuit boards or organic electronic substrates. Chen, Fu and coworkers successfully produced amine-functional BNNT via ball-milling using an aqueous urea solution without damaging the crystalline structure and dimension of the BNNS and used simple vacuum-assisted filtration for the production of a composite film based on cellulose nanofibers (Figure 6A) (Wu et al., 2017). The in-plane thermal conductivity of 70 wt % f-BNNS containing cellulose nanofiber composite with a thickness of ~90 μm reached to 12.79 W m^{-1} K^{-1}, which is almost 1.7 times higher than neat BNNS containing cellulose nanofiber composite with same conditions and 8 times higher than pure cellulose nanofibers. The value increased up to

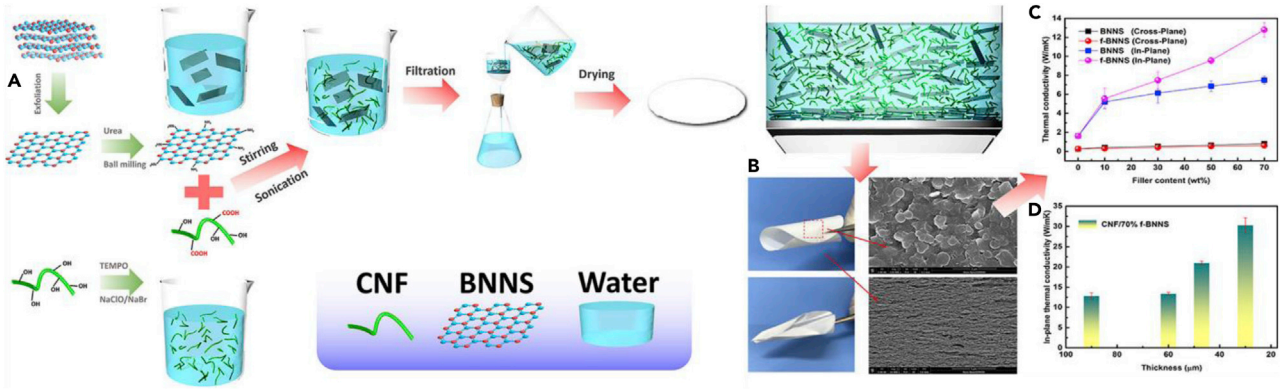

Figure 6. Preparation of biodegradable CNF/f-BNNS film with high thermal conductivity and flexibility

(A–D) (A) Schematic illustration for the production of CNF/f-BNNS composite film, (B) photographs, surface and cross-plane morphologies of the composite films, (C) in-plane and cross-plane thermal conductivities of the composite films, (D) in-plane thermal conductivity of the composite film as a decrease of the thickness. Adapted from Wu et al. (Wu et al., 2017) with permission from ACS Publishing Group.

30.25 W m^{-1} K^{-1} at the thickness of ~30 μm, suggesting both the effect of functionalization and higher orientation with thinner films (Figure 6C). The composites also had better tensile strength, elongation, and flexibility and lower dielectric constant than pure cellulose nanofibers. These properties make the f-BNNT/cellulose nanofiber composites ideal candidates for electronic devices.

The same group also produced an edged hydroxylated BNNTs (EOH-BNNT) via ball milling, which preserved the lattice structure and transformed to BNNT/cellulose nanofiber composites via vacuum filtration (Wu et al., 2018). POH-BNNT/cellulose nanofiber composites increased the thermal conductivity only by 10% compared with neat BNNT/cellulose nanofiber composites, whereas EOH-BNNT composites resulted in a 97.8% enhancement, reaching a value of 24.27 W m^{-1} K^{-1}. EOH-BNNT/cellulose nanofiber composites also show better hydrophobic property, flexibility, and tensile strength, which are promising materials for portable electronic devices. In a study by Fu et al., the improvement in the thermal conductivity of BNNT-based composites was studied via decreasing the interfacial thermal resistance between BNNTs, which is provided by creating bridges between BNNTs with the help of silver nanoparticles (Fu et al., 2018). Ag-BNNT/CNF composites were prepared via vacuum filtration and hot-pressing. The thermal conductivity of Ag-BNNT/CNF composite reached to its maximum as 20.9 W m^{-1} K^{-1} with 25 wt % BNNT and 0.199 wt % Ag, compared with 1.45 W m^{-1} K^{-1} of the pure CNFs, which also maintained its thermal stability after 30 heating/cooling cycles. In a recent study by Zhang and coworkers, h-BN/PS nanocomposites were prepared by the *in situ* polymerization of carboxylated PS on hydroxylated BNNS, followed by vacuum filtration and hot-pressing (Han et al., 2020). The thermal conductivity of the obtained PS-COOH/BNNS-OH/PS composites arrived at 1.131 W m^{-1} K^{-1} with 12 wt % BN-OH addition, which is 6.1 and 3.6 times higher than pure PS and unmodified BN/PS composites due to the noncovalent interactions between PS-COOH and BN-OH. With good thermal conductivity, stability, thermal response behavior, and mechanical properties, these composites are potential as thermal interface materials in heat dissipation applications as cooling devices. In a recent study, Xu and coworkers prepared BNNS/ethylene-vinyl acetate copolymer (EVA) composite films via vacuum-assisted self-assembly, following the formation of BNNS from h-BN through eco-friendly biomolecule-assisted exfoliation (Wang et al., 2020). The in-plane thermal conductivity of the BNNS/EVA reached to 13.2 W m^{-1} $K^{-1}$with 50 wt % BNNS, which is 71% higher than that of 50 wt % BN/EVA as a result of the orderly structure of BNNS. The composite films were highly flexible, retaining the structure and thermal conductivity after 5,000 bending cycles, highlighting their potential in thermal management applications.

Coating with nanofillers

Coating process includes the deposition of one or multiple layers of fillers on the surface of a material aiming to produce a uniform and stable coating with sufficient thickness and adhesion to the surface (Shim, 2019; Huang et al., 2021; Fu and Yu, 2014). There are various coating techniques depending on the coating material, substrate, end-performance, and costs. Dip-coating is a simple technique suitable for scaling-up. However, the process occurs at both sides of the substrate, which may not be suitable for all applications. Knife-over-roll and doctor-blading methods are also fast, scalable, and low-cost methods, but they have

drawbacks such as low reproducibility and uniformity. Electrophoretic deposition (EPD) is an easy method to produce functional coatings based on the use of the deposition of charged particles/molecules in a solvent on oppositely charged particles through electric field-assisted migration. It is a cost-effective and scalable method with high versatility but it suffers from the need of a stable suspension and sufficient particle charge and undesirable electrochemical reactions (Saji, 2021).

Coating with carbon-based nanofillers

Rahman and Mieno coated cotton fabric with multiwall carbon nanotubes functionalized by oxygen-containing surface groups (*f*-MWCNTs) via simple dipping-drying technique (Rahman and Mieno, 2015). The *f*-MWCNTs/cotton fabric became electrically conductive after dipping in the dispersion for 10 times, whereas its thermal conductivity also increased to 0.045 W m^{-1} K^{-1} from 0.027 W m^{-1} K^{-1} for unmodified cotton. The thermal stability and flame retardancy of the *f*-MWCNTs/cotton fabric were also improved. Cotton was coated separately with graphene, MWCNT, and BN dispersions in a resin via dip-pad-cure technique by Lin and coworkers (Abbas et al., 2013). Morphologically, MWCNT had a fibrous structure, and uniform distribution on the cotton, the graphene-coated fiber, had a smooth surface, whereas their surface became rougher with BN coating. The thermal conductivity of the coated cotton increased in the order of graphene > BN > MWCNT at the same coating content, reaching to a maximum of 0.29 $\pm$ 0.015 W m^{-1} K^{-1} with 50 wt % graphene coating. Graphene also provided a better heat dissipation than BN and MWCNT but lower air permeability. In a study by Tian, Qu and coworkers, graphene oxide nanosheets were deposited onto plain woven polyamide fabric by EPD followed by hot-pressing (Zhao et al., 2018a). Under the optimal EPD conditions (deposition time of 150 s and voltage of 10 V), the electrical conductivity of the polyamide/rGO composite fabric increased to 3.3 S/m, whereas the thermal conductivity of the polyamide/rGO composite fabric increased to 0.521 W m^{-1} K^{-1}, which is about 175% higher than that of the control fabric. These hydrophobic composite nanofibers are promising for smart wearable devices. Ulcay and colleagues demonstrated electrically and thermal conductive textiles surfaces by homogeneously coating pretreated polyester fabrics with nano graphene powders (Manasoglu et al., 2019) and GNPs (Manasoglu et al., 2021) by knife-over-roll technique. Thermal conductivity of the nano-graphene-coated polyester fabrics increased with increasing graphene concentration with a highest value of 0.4243 W m^{-1} K^{-1} for 200 g/kg graphene concentration rate, corresponding to 304.5% increase compared with uncoated fabric, whereas it reached to 0.492 W m^{-1} K^{-1} with GNP coating of 0.5 mm thickness and 150 g/kg concentration. The solar absorbance values of graphene-coated fabrics increased by 83.72 and 80.12% for 0.1 and 0.5 mm thickness, respectively. Plain weave bamboo viscose fabrics were coated with graphene/cellulose nanocrystal (G/CNC) dispersions using dip-coating method in a work by Yang et al. (2019) Thermal conductivity of G/CNC-coated bamboo fabric reached to 0.136 W m^{-1} K^{-1} with 4 wt % CNC and 3 wt % G, whereas it was around 0.049 W m^{-1} K^{-1} for CNC-coated bamboo fabric, due to the uniform distribution of G and hydrogen interactions between bamboo and G, indicating the potential of the coated bamboo fabric as cooling textiles, conductive fabrics, and wearable electronics. Zhang and colleagues followed a different path for producing conductive textiles based on a green method, which included the dip-coating of a 70% polyester-30% cotton with an aqueous dispersion of MWCNT, graphene, and hydroxyl terminated PU (WPU) as shown in Figure 7 (Dai et al., 2021). The electromagnetic interference shielding effectiveness (EMI SE) of the coated textile reached to 35 dB at the thickness of 0.35 mm with a filler amount of only 3%. Hybrid fillers of CNT and graphene increased the thermal conductivity from 0.075 W m^{-1} K^{-1} to 0.704 W m^{-1} K^{-1} while also improving mechanical properties and thermal stability. These conductive textiles opened an avenue for advanced EMI shielding applications.

A recent research by Zhao and Liu showed that polyaniline/graphene composite coating improved the dielectric property, mechanical properties, and thermal stability of the polyester fabric (Liu and Zhao, 2021). The thermal conductivity coefficient of the coated polyester fabric also increased from 0.1011 W m^{-1} K^{-1} to 0.1843 W m^{-1} K^{-1} when the graphene content was 15% that of the polyaniline, compared with only polyaniline coated polyester. Das and coworkers designed a merino wool/nylon (W–N)-based multifunctional textile by coating the W-N with a phase-separated PEG/PEDOT:PSS/rGO suspension via dipping-drying method (Ghosh et al., 2020). The PEG/PEDOT:PSS/rGO/W-N textile reached a DC electrical conductivity of 90.5 S cm^{-1}, EMI SE of 73.8 dB in the X-band frequency domain, and in-plane thermal conductivity of 0.81 W m^{-1} K^{-1} with 20 dipping cycles and a thickness of 0.84 mm. The designed e-textile was tested to be an EM protective cloth combined with real-life antenna performance, a TASER Proof Textile and photoluminescent wearable e-textile. In a recent study by Bonetti et al., GNP/PU nanocomposite membranes were prepared via blade-coating in order to improve thermal comfort in functional textiles (Bonetti et al., 2021). A remarkable increase of 471% in the

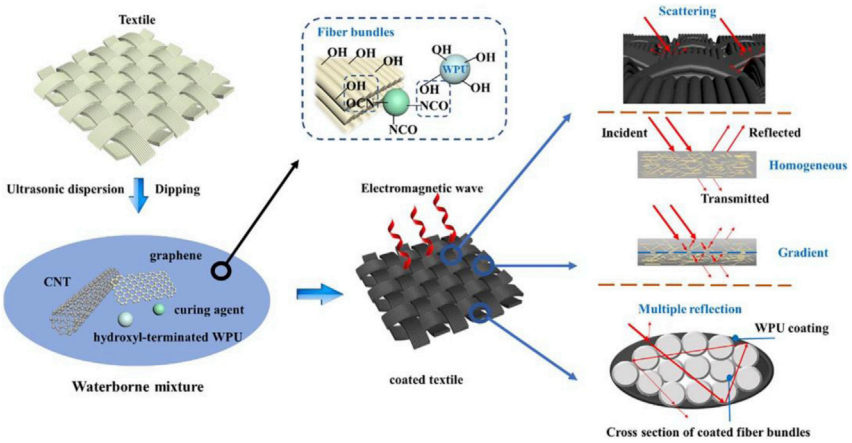

Figure 7. Schematic illustration of EMI SE mechanisms for bilayers/textile
Adapted from Dai et al. (Dai et al., 2021) with permission from Elsevier Publishing Group.

thermal conductivity of GNP/PU composite was achieved with an addition of 10 wt % GNP, reaching a value of 6.28 W m^{-1} K^{-1}. The thermal testing of both the GNP/PU nanocomposites and their coupling to cotton fabric were performed on a manikin setup of human forearm simulating an athlete under outdoor aerobic effort, which indicated their efficiency in heat dissipation. The GNP/PU nanocomposites show great potential in the design of new functional textiles as they can be easily coupled to textiles for improved thermal properties. Soong and Chiu introduced GNP- and BN-containing TPU multilayered composite films to be used for cooling garments (Soong and Chiu, 2021). GNP and BN were separately mixed with TPU via mechanical mixing, which were then poured to form a multilayered structure via blade coating. The thermal conductivity of the composite film with 20 wt % GNP and 20 wt % BN was increased to 6.86 W m^{-1} K^{-1} corresponding to an increase of 2,844%, 143%, and 62% compared with neat TPU, GNP(20%)/TPU, and BN(20%)/TPU films, respectively. The cooling performance of the composite film was evaluated by attaching it to the inner side of a t-shirt that has an active cooling source on the outer surface. Active cooling performance measurements demonstrated that the active cooling source was able to increase the spreading of the cool air and transfer the air to the skin through the BN-GNP/TPU film. With ability of cooling, durability in fatigue, and laundry tests, these composite films are promising candidates as thermal interface materials within smart cooling garments.

Coating with boron-based nanofillers

In a recent study by Sun and coworkers, a BNNS-containing TPU film was manufactured via ultrasonication and doctor blading and was covered with a graphene nanoribbon (GNR)-decorated TPU nanofibrous scaffold fabricated via vacuum filtration of GNR dispersion through electrospun TPU membrane (Tan et al., 2020). The resulting highly stretchable, breathable, and biocompatible strain sensor with 35 wt % BNNSs and 50 μg cm^{-2} GNRs had a thermal conductivity of 0.928W m^{-1} K^{-1} with a high interfacial thermal conductance of 2.9 × 10^4 Wm^{-2} K^{-1} between the TPU-BNNS film and air. The strain sensor showed stability for more than 5,000 cycles as well as vapor permeability, breathability, and biocompatibility, which is important for direct human skin-attachable applications. Tian and coworkers introduced shear-oriented BNNS/CNF by doctor-blading method via mechanical shear-induced orientation with filler content of 0–50 wt % (Chen et al., 2019b). The thermal conductivity of the shear-oriented BNNS/CNF composites was increased to 24.66 W m^{-1} K^{-1}, which corresponds to 1,106% enhancement in comparison with the pure CNF as a result of high orientation degree of BNNS. The improved thermal stability, conductivity, and good dielectric properties put forward these composites as valuable prospects for flexible microelectronic packaging.

Spraying of nanofillers

Spraying method includes the use of an airbrush to spray a solution containing the fillers to a preheated substrate, leaving membranes modified with the fillers after solvent evaporation (Cheng et al., 2017). The spray gun serves to disperse and form fine droplets of the spray solution. Electro-spray uses high electric potential to charge the droplets fed through a nozzle. The spraying method can be applied on various types of substrates with negligible material loss, high scale-up capacity, and satisfying accuracy of properties control; however, the uniformity of the membranes may be poor in homogeneity.

Spraying of carbon-based nanofillers

Gasthi and colleagues prepared graphene/polyvinylphosphonic acid/cotton nanocomposite via layer-by-layer spray coating that consisted of alternating sprays of acid-functional graphene/surfactant and vinylphosphonic acid/initiator dispersions, followed by thermal curing (Nooralian et al., 2016). The coatings were found to increase the hydrophobicity, thermal stability, electrical conductivity, UV absorption, and EMI shielding of the graphene/polyvinylphosphonic acid/cotton nanocomposites compared with neat cotton. Yu et al. uniformly coated an aldehyde-modified cotton fabric with an MWCNT fluid via spraying (Yu et al., 2019). The nanofluids are considered as flexible heat transfer materials to fabricate high heat transfer coating. So, it was not surprising that the thermal conductivity of MWCNT-fluid-coated cotton fabric improved to 0.213 W m^{-1} K^{-1} as a result of the strong network structure, whereas that of the aldehyde-modified cotton was measured as 0.088 W m^{-1} K^{-1}.

Wang and Cai combined spraying and vacuum-assisted resin transfer infusion process to develop a GNP/carbon fiber/epoxy composite. A solution containing GNP, epoxy, and hardener was sprayed on dry carbon fabrics, followed by the formation of a composite structure with eight layers of the reinforced fabric and epoxy (Wang and Cai, 2019). The increased surface area, uniform and dense deposition of GNPs, and good interfacial adhesion between fiber-matrix increased the thermal conductivity of the GNP/fiber/epoxy composites to 0.84 W m^{-1} K^{-1} after 0.5 wt % GNP addition compared with 0.54 W m^{-1} K^{-1} of the pristine composites, also improving the mechanical properties.

Spraying of boron-based nanofillers

Huang and coworkers brought in a different strategy inspired from a millefeuille, producing multilayer nanonetwork structures by spraying BNNS onto electrospun poly(vinyl alcohol) (PVA) nanofibers with average diameter of 300–400 nm, followed by cutting the layer into small pieces, overlaying them layer-by-layer and thermally molding (Chen et al., 2019c). The PVA/BNNS nanocomposite with 33.1 wt % BNNS and spraying time of 80 min reached an in-plane thermal conductivity of 21.4 W m^{-1} K^{-1}, which is 100 times higher than that of the pure PVA, due to the oriented BNNS and overlapping interactions. The composites maintained their thermal conductivity even at 90ºC after multiple heating-cooling cycles, as well as being insulator. Overlaying also contributed to the efficiency of heat dissipating compared with randomly dispersed BNNS or directly hot-pressed BNNS composites, making these multilayered PVA/BNNS nanocomposites attractive as high-performance lateral heat spreaders.

Wet spinning

Thermally conductive and electrically insulating BN nanopowder (BNNP)/PU composite fibers were wet-spinned by Wallace and coworkers (Farajikhah et al., 2019). The addition of BNNP resulted in a decrease in specific heat capacity and increase in thermal diffusivity and thermal conductivity, which improved around 160% with a low loading of 5 wt % BNNP, reaching 0.262 W m^{-1} K^{-1}. These composite fibers with additional improved mechanical properties could be successfully integrated into a 3D knitted polyester structure via a tubular knitting technique, pointing out the feasibility of these composite fibers. In a recent study, Fu and coworkers produced regenerated cellulose (RCF)/BNNS multifilaments with average diameters of 50–100 μm via wet spinning of an aqueous solution of biodegradable cellulose and edge-selective hydroxylated BNNSs produced by ball milling (Wu et al., 2019). The thermal conductivity of the composite filaments increased to 1.682 W m^{-1} K^{-1} with 60 wt % BNNS with random distribution, whereas it reached up to 2.914 W m^{-1} K^{-1} with increase in the drawing ratio of the RCF/BNNS filaments (H-RCF/BNNS) under the same conditions due to enhanced orientation. These filaments also displayed superior hydrophilic property and stable hygroscopic performance as well as good mechanical properties and high heat radiation emittance, which are suitable for applications of personal cooling in the case of sporting. Wet spinning has the advantage of suitability to a wide range of polymers with continuity and offers scalability; however, it can suffer from the use of volatile and cytotoxic solvents, as well as low production rate, higher manufacturing costs, and difficulty in scaling-up (Wei et al., 2021). Moreover, if the drawing process cannot be well controlled, the fibers can dry too quickly at room temperature, leading to defects in molecular orientation.

3D printing

3D printing, or additive manufacturing is a process of joining of materials such as plastics, liquids, or powder grains typically layer by layer in order to construct three-dimensional (3D) objects using a

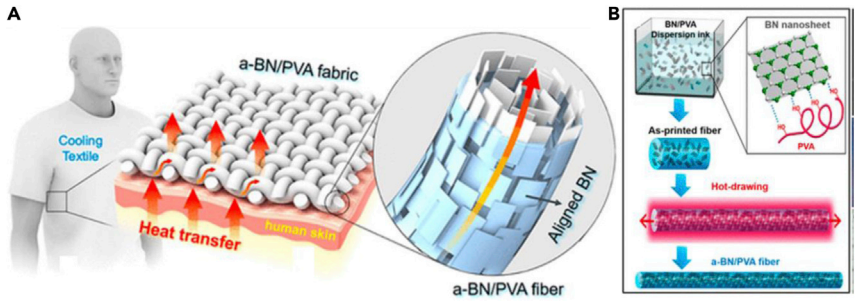

Figure 8. Wearable thermal regulated textiles composed of 3D-printed a-BN/PVA fibers for personal cooling
Schematic illustrations of (A) the thermal regulation textile, (B) the production of a-BN/PVA composite fiber. Adapted from Gao et al. (Gao et al., 2017) with permission from ACS Publishing Group.

computer-aided design software (Ngo et al., 2018). Various printing techniques such as fused deposition modeling, selective laser sintering, inkjet 3D printing, stereolithography, and 3D plotting have been developed to fabricate polymer composites. 3D printing allows the fabrication of polymer composites with high mechanical properties and functionality by incorporating particles, fibers, or nanomaterial reinforcements. 3D printing has several advantages such as reduced waste during the fabrication of composite structures, precise control of the size and shape of the composites, process flexibility, cost-effectiveness, and environmental friendliness. However, the materials suitable for 3D printing are limited and the raw materials are expensive, whereas scaling-up is not cost-effective.

In a study by Hu and coworkers, a personal thermo-regulating textile was fabricated by aligned BN and PVA composite fibers that were obtained via 3D printing, followed by hot-drawing, for further orientation of the BNNS (Figures 8 A and 8B). (Gao et al., 2017) The thermal conductivity of the resultant BNNS/PVA fabric increased to 0.078 W m^{-1} K^{-1}, which is 2.2 and 1.6 times more than that of the cotton fabric and PVA fabric, respectively. The cooling effect of the composite fabric was also found to be 55% greater than the cotton fabric in addition to the enhanced tensile strength and stiffness. This wearable BNNS/PVA textile draws attention for personal cooling, which is more economical and eco-friendly than cooling an entire building. The primary advantage of this method is material flexibility. Solutions, pastes, and hydrogels can all be loaded into 3D plotting printers; however, the mechanical strength and production speed can be low (Wang et al., 2017).

Cai and coworkers prepared flexible filaments of polylactic acid/wheat flour/thermoplastic polyurethane composites with nano-graphite via fused deposition modeling (Guo et al., 2019b). The thermal conductivity of the composites rose with increasing graphite content, reaching around 0.32 W m^{-1} K^{-1} with 30% graphite due to the conductive network that also improved mechanical properties and thermal stability. For further modification of the composites, rGO, tannic-acid-functionalized graphite, or MWCNTs were added, which respectively increased the thermal conductivity to 0.44 W m^{-1} K^{-1}, 0.47 W m^{-1} K^{-1}, and 0.38 W m^{-1} K^{-1}. The disadvantage of fused-deposition printers is that the raw material is limited to thermoplastic polymers with molten viscosity high enough to support the structure and low enough to permit extrusion, in addition to the possibility of nozzle clogging (Wang et al., 2017).

Chemical coupling of nanofillers

Chemical coupling of carbon-based nanofillers

Yu and coworkers used the thiol-ene chemistry for the production of thermally conductive polyester fabric (Zhao et al., 2018b). A thiol-modified polyester fabric was placed in a dispersion of a dien-containing PEG-based hydrophilic finishing agent and a thiol-containing reduced graphene oxide under UV irradiation. Analyses pointed out the advance both in the thermal conductivity and moisture management properties, which makes the modified fabric promising for usage in daily and sportswear. The same group also prepared a thiol-modified rGO-waterborne PU/cotton (M-rGO-WPU/cotton) fabric with improved EMI shielding and thermal conductivity (Wang et al., 2019). WPU with ene groups at both ends was reacted with thiol-modified cotton and thiol-modified rGO via synchronous thiol-ene click reaction, which resulted in a uniform attachment of rGO onto cotton. The thermal conductivity of M-rGO-WPU/cotton increased to 2.13 W m^{-1} K^{-1}, which is about 3.67 times higher than that of cotton. The EMI shielding of M-rGO-WPU/cotton could be maintained upon 1,000

cycle bending, 10 cycles of washing, and friction. Moreover, the material is lightweight and easily processable with improved electrical and mechanical properties as well as high heat transfer efficiency, highlighting its suitability for advanced EMI shielding applications with all these superior properties.

Chemical coupling of boron-based nanofillers

Kim and coworkers investigated both physical and chemical assembly of amine-functionalized BNNTs onto electrospun polyacrylic acid/polyvinyl alcohol nanofibers for enhancing the thermal conductivity (Kim et al., 2018). With the chemical assembly of 1 wt % BNNTs, the thermal conductivity and thermal diffusivity, respectively, increased to 0.65 W m^{-1} K^{-1} and 9.01 10^{-7} m^2 s^{-1}, which are 1.5-fold to that of neat PAA/PVA nanofibers due to the covalent bonding, whereas physical assembly only showed a negligible improvement. These thermally improved polymeric composites can be used for applications such as sensing and catalysis.

Miscellaneous

Ding and coworkers announced a novel green plastic composed of cellulose fiber and functionalized graphene for high-performance thermal management devices with improved thermal conductivity through hot-pressing of a cellulose/graphene hydrogel (Song et al., 2017). The in-plane thermal conductivity of the produced composite bioplastic reached to 9.0 W m^{-1} K^{-1} with 6 wt % of graphene, whereas that of the neat cellulose bioplastic was 2.59 W m^{-1} K^{-1}. The composite plastic also has improved thermal stability, mechanical properties as well as superior thermal dissipation and high flexibility. The production of thermal interface materials from bio-based and renewable resources was reported by Bayer and coworkers via loading GNPs in regenerated cellulose by bath sonication and solution casting, followed by hot-pressing (Zahid et al., 2018). At 25 wt %, GnPs formed a dense and interconnected network on the film with cross-plane and in-plane thermal conductivities around 5.5 W m^{-1} K^{-1} and 800 W m^{-1} K^{-1}, respectively, based on chip-stack inspired experimental methods. In addition to these thermal properties, the electrical conductivity of 30 S/m and good mechanical properties pave the way for these renewable composites as thermal interface materials. Windle and coworkers introduced CNT microfibers via floating catalyst chemical vapor deposition (Gspann et al., 2017). The thermal conductivities of the CNT films were measured as 110 W m^{-1} K^{-1} by the parallel thermal conductance method, whereas that of the CNT microfibers was 770 W m^{-1} K^{-1}, due to the high degree of alignment. Marconnet and colleagues developed a steady state thermal conductivity measurement technique based on infrared microscopy and measured the thermal conductivity of ultrahigh molecular weight polyethylene (UHMW-PE) in the forms of individual microfiber of 20 μm as 28.4 ± 3 W m^{-1} K^{-1}, yarn from twisting of the fiber with a diameter of ∼370 μm as ∼ 16 W m^{-1} K^{-1}, and woven fabric with a width and thickness of ∼2.1 mm and ∼660 μm as 9.5 ± 0.6 W m^{-1} K^{-1} (Candadai et al., 2020). Upscaled woven UHMW-PE fabrics with high thermal conductivity can be prepared for heat spreading applications. Li et al. used a three-step procedure to fabricate graphene fiber fabrics, including spinning and drying of graphene oxide staple fibers, wet-fusing assembly into fabrics, and high-temperature annealing/reduction at 3,000 ºC (Li et al., 2016b). The resultant nonwoven fabric was composed of randomly oriented and interfused graphene fibers with strong interfiber bonding, overcoming the limited performance of conventional carbon fibers with weak interfiber interactions. The electrical and thermal conductivities of the nonwoven graphene fabric reached to 2.8 × 10 S m^{-1} and 301.5 W m^{-1} K^{-1}, respectively. Poly(3-hydroxybutyrate-co-3-hydroxyvalerate) (PHBV) hybrid composites were prepared with three different hybrid systems, namely hexagobal-boron nitride/graphene tube (h-BN/GT), aluminum nitride (AN)/GT, and h-BN/aluminum oxide (AO) via compression molding and hot-pressing by Azlan and colleauges (Vishnu Chandar et al., 2021). Measurements via hot disk instrument pointed out that the maximum thermal conductivity reached was 0.5215 W m^{-1} K^{-1} upon addition of AN/GT with 0.5/1.5 filler concentration, compared with neat PHBV matrix (0.2303 W m^{-1} K^{-1}). These bio-based PHBV hybrid composites are promising in UV-shielding textile fabric coating, as well as in apparel applications in the spun form with improved thermal and mechanical properties.

Ding and coworkers took inspiration from the temperature control principle of a butterfly for a novel route for smart thermal management. Both mono (U-G/PEG/NFC), bilayer hybrid films (B-G/PEG/NFC) (Cui et al., 2019), and 5-layered G/PEG/NFC hybrid film (Song et al., 2021) consisting of graphene sheets, PEG, and nanofibrillated cellulose were prepared via evaporation-induced self-assembly process, followed by hot-pressing for 5-layered film as shown in Figure 9A. The in-plane thermal conductivity of the B-G/PEG/NFC hybrid film with 30 wt % graphene increased to 21.83 W m^{-1} K^{-1}, which is 31.11% higher than that of the U-G/PEG/NFC hybrid film due to the thermally conductive pathway created by denser graphene

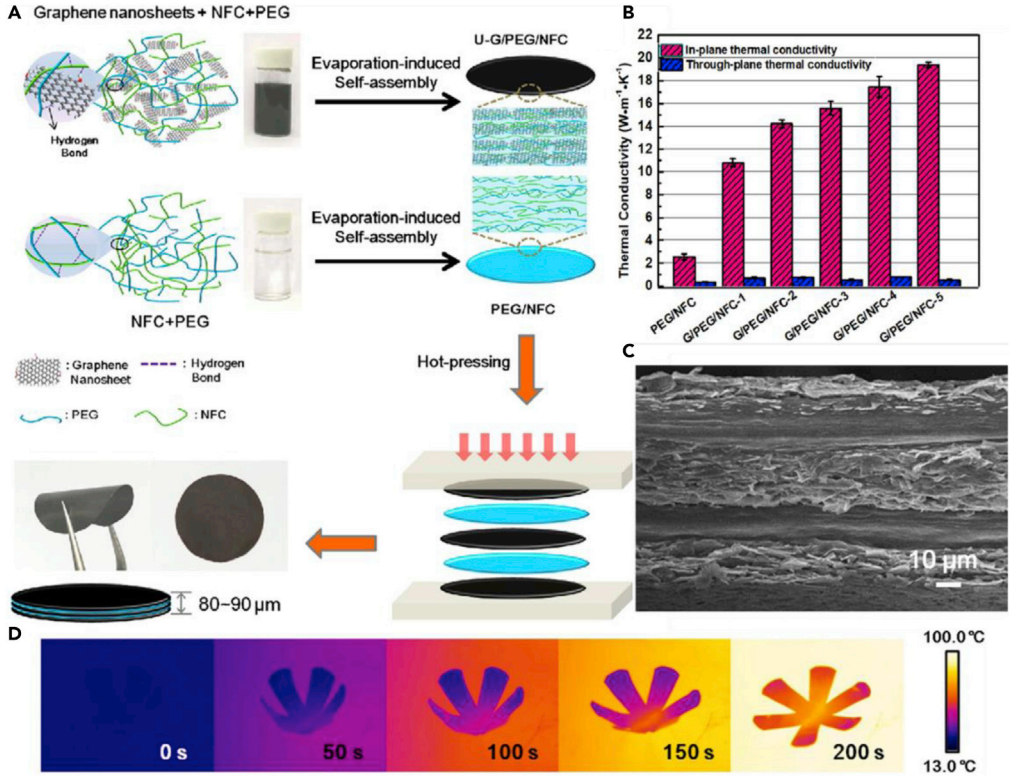

Figure 9. Multilayered flexible G/PEG/NFC hybrid film with thermally activated shape memory property designed for thermal management

(A–D) (A) Schematic illustration of the fabrication process, (B) thermal conductivities, (C) SEM image of cross-sectional view, (D) infrared thermal images for shape recovery processes of 5-layered G/PEG/NFC hybrid film. Adapted from Song et al. (Song et al., 2021) with permission from Elsevier Publishing Group.

packing. Over the melting point of PEG, the flower shape was folded into bud shape temporarily, which turned back to the original shape in an oven at 70 °C in 40 s for PEG/NFC, 28 s for U-G/PEG/NFC, and 14 s for B-G/PEG/NFC, as a result of the shape memory property of PEG. The thermal conductivity of the 5-layered with 20 wt % graphene was measured as 19.37 W m^{-1} K^{-1}. The active heat dissipation response property of the films was evaluated by an LED system by retarding the heating of LED and visually informing when temperature of LED exceeds a certain value via shape change between bloom and bud (Figure 9D), providing inspiration for future development in smart thermal management.

Ouyang and coworkers prepared rGO/CNT-containing composite textile composed of nano-soldering of CNTs into a polypropylene/viscose nonwoven fabric (NWF) followed by rGO deposition via chemical reduction of GO (Tang et al., 2020). The fabricated rGO/CNT/NWF possessed a thermal conductivity coefficient of 2.90 W m^{-1} K^{-1}, whereas that of the neat nonwoven was 0.03 W m^{-1} K^{-1}, which was attributed to the synergetic effect of rGO and CNT, as rGO sheets can rise the thermal conductivity through bridging the CNTs. High thermal conductivity and good mechanical properties together with high machine washability demonstrated the suitability of the rGO/CNT/NWF composites as wearable sensors.

Recently He and Wang presented thermally improved flexible PI composite films using the dual fillers, GO nanosheets, and h-BN platelets (He and Wang, 2020). At first, poly(amide acid) (PAA)/BN solution was prepared via *in situ* polymerization. Then, GO was uniformly dispersed in the PAA/BN solution, followed by casting and thermal treatment to end with PI/BN/GO composite film. The thermal conductivity of the PI/BN/GO composite film increased to 11.203 W m^{-1} K^{-1} at a low filler loading of 1 wt % GO and 20 wt % BN, which is 50 times higher than that of neat PI due to the percolation effect of the binary fillers. With improved thermal mechanical properties, thermal stability, dielectic properties, and insulation, PI composites can be used for thermal management applications.

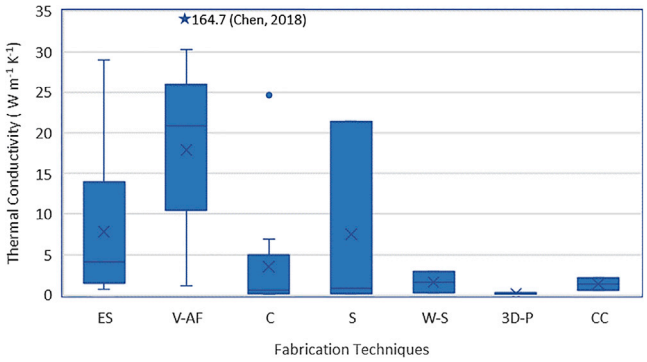

Figure 10. The thermal conductivity ranges corresponding to the fabrication techniques
(ES, V-AF, C, S, W-S, 3D-P and CC refer to electrospinning, vacuum-assisted filtration, coating, spraying, wet-spinning, 3D-printing, and chemical coupling, respectively).

CONCLUSIONS

Textile fabrics are advantageous materials due to properties such as high surface area, flexibility, and mechanical properties that make them attractive substrates for the integration of conductive materials. Heat conduction control is important in order to increase or decrease human body heat loss. Conduction is the only pathway for the dissipation of heat within a textile materials and the leading way for heat transport between the skin and the inner surface of clothing for IR-opaque textiles. Novel textile materials are worth to be designed for improved personal thermal management and thermal comfort. In this review, we focused on enhancing the thermal conductivities of materials mainly via passive conductive warming/cooling for thermal regulation. We investigated the enhancement in thermal conductivity in terms of fabrication techniques and filler types, mainly focusing on carbon-based fillers and boron-based fillers. The improvement in the thermal conductivity of the materials depended on several parameters such as fabrication process, material structure, material form, type, and amount of fillers. A summary of the maximum achieved thermal conductivities depending on the fabrication method and nanofiller type is given in Table 1, as well as a thermal conductivity versus fabrication method box-plot in Figure 10. The choice of the fabrication process can be decided based on the needs in terms of the amount, yield, and required thermal conductivity. For instance, electrospinning is a simple and efficient method for producing thermally improved materials; however, it is not efficiently scalable for industrial production. In addition, the produced nanofiber surfaces are delicate materials to be used as clothing, so they can be used as reinforcement layers. Vacuum filtration is indeed a simple and eco-friendly method that can easily control the thickness of the filler layer, but it is difficult to fabricate a large-area membrane. Spraying has the advantage of applicability to any substrate, and it can be preferred for large-area surfaces; however, the uniformity might be unfulfilling. Coating is a plausible technique for the modification of fabrics with conductive fillers. Both dip-coating and pad-dry are simple, scalable, and cost-effective methods, but they coat both sides of the material, so they can be more suitable for the production of wearable e-textiles. Doctor blading and knife-over-roll are also inexpensive, productive, and scalable without losing uniformity with scaling, These methods are not suitable for very thin layers of coating, which can instead be achieved by layer-by-layer assembly. According to Table 1, the thermal conductivities achieved by electrospinning varied between 0.689–29 W m^{-1} K^{-1}, depending on the presence and type of the nanofiller. Vacuum-assisted filtration method gave a wide range of thermal conductivities between 1.131–164.7 W m^{-1} K^{-1} subject to type and amount of the nanofiller and reached to its maximum value with addition of 50 wt % graphene to cellulose nanofiber. In coating, dip-coating, dip-pad-cure, and knife-over-roll methods slightly improved the thermal conductivity. The maximum value reached among the coating techniques was 24.66 W m^{-1} K^{-1} using doctor blading method for the coating of cellulose nanofiber with 50 wt % BNNS content. Spraying of MWCNT and GNP on cotton and epoxy, respectively, increased the thermal conductivities to 0.213 W m^{-1} K^{-1} and 0.84 W m^{-1} K^{-1}, whereas spraying of BNNS (33.1 wt %) on PVA nanofiber for 80 min improved the thermal conductivity to 21.4 W m^{-1} K^{-1}. Wet spinning of regenerated cellulose with 60 wt % BNNS raised the thermal conductivity to 1.682 W m^{-1} K^{-1} and to 2.914 W m^{-1} K^{-1} after extra drawing. 3D printing of PVA with BNNS and FDM of PLA with nano-graphite reached only to 0.078 W m^{-1} K^{-1} and 0.32 W m^{-1} K^{-1}, respectively. Chemical coupling of PU and cotton with rGO via thiol-ene reaction resulted in a thermal conductivity of 2.13 W m^{-1} K^{-1}.

Figure 10 also demonstrates the thermal conductivity ranges depending on the fabrication methods. The graph indicates that the maximum thermal conductivities were reached by vacuum-assisted filtration and spraying, followed by electrospinning. It can be clearly seen that wet spinning, 3D printing, and chemical coupling did not significantly improve the thermal conductivity. It is important to note that all these methods are valuable, as in some cases textiles with low thermal conductivities are needed, whereas for some applications textiles should have high thermal conductivities.

FUTURE PERSPECTIVES

The thermal conductive textiles have a wide range of application areas including outdoor apparel clothing, home thermal products, medical apparel, and treatments. Home textiles such as smart thermal mattresses, sheets, and pillowcases can offer thermal treatment as well as energy saving. The personal cooling that can be achieved by clothing with improved thermal conductivity also contributes in saving energy, conditioning cost and reducing greenhouse gas emissions. Carbon-filler-based fabrics also show insulation property, as graphene and CNTs keep heat well and spread it uniformly in cold weathers, also retaining the body temperature stable in cold environment and during physical activity. According to these properties, the graphene-based textiles are also used in outdoor sportswear, ski wear, and military clothing, as well as post-surgery, maternal, and new-born clothing where heat transfer from hot parts of the body to the colder parts of the body is favorable. In addition, graphene is antimicrobial showing cytotoxicity to bacteria, so graphene-based fabrics have practical applications in hospital clothing and maternity clothes. In addition to these remarkable thermal properties, the ability of graphene-based materials in distributing the impact force, their lightweight and improved ballistic properties make them suitable materials for military applications such as lighter and more comfortable military uniform, armor, and helmets (Mittal et al., 2018). Advances in thermal camouflage technologies can also be developed using radiative and conductive strategies (Hu et al., 2021). The increase in thermal conductivity with the use of these graphene- and boron-based materials contribute in the spreading of heat and passive cooling as well as storing thermal energy, influencing human skin lesser and diminishing burn injuries. So, they are suitable for clothing of fire fighters, hazmat, and health care workers, military/police personnel and cooling vests, and emergency blankets (Bhattacharjee et al., 2019). The flame-retardancy property of boron nanosheets is also used in outdoor equipment such as tents (Yaras et al., 2016).

Graphene- and boron-based textiles have potential for wearable technologies, as they are able to enhance wear resistance, tearing, flexibility, piezoresistivity, and thermal and electrical conductivities (Wang et al., 2021; Abu-Thabit et al., 2016). Such unique properties propose their use in smart textiles, wearable electronics, strain sensor, health monitoring, stretchable solar cells, supercapacitors, and field emission devices. Research has focused on human warming and cooling clothing, wearable sensors, antennas, intelligent textile, energy storage, and portable electronic devices. The use of the conductive materials as flexible lithium-ion batteries and conductors has also been studied as a power source for flexible and wearable electronic devices such as roll-up displays, touch screens, wearable sensors, and medical implants, as they are able to improve charge rate capability and cyclic stability. Conductive-textile-based energy storage systems, supercapacitors, and Li-ion batteries are attractive alternatives to conventional heavy and rigid parts for the production of novel energy products such as e-vehicles. These systems are light, flexible, and miniaturized, contributing in fuel-saving and reducing CO_2 emissions. The EMI SE property of the conductive materials opens up application areas such as antennas and frequency shielding coatings for aircraft and electronics.

Soft and flexible thermal interface materials (TIMs) that are designed to have high thermal conductivity, heat dissipation ability, and electromagnetic interference shielding effectiveness with miniaturized sizes can be promising for 5G applications. Internet of Things (IoT) is another technology based on connecting everything wirelessly, which is expected to be developed after wider spreading of 5G networks (Rahman et al., 2019; Paracha et al., 2019). Wearable devices used in various applications such as fitness, medical, entertainment, and rescue are also prepared for being a part of IoT. Research is in progress on combining IoT technology on personalized textile thermoregulation based on autonomously collecting data and respond to the changes in the micro- and macro-environment of body via optimized active and passive thermoregulation strategies (Chen et al., 2021).

Next-generation smart fabrics demand for adaptability to the exterior environment with efficient heating and cooling features in addition to conventional requirements such as flexibility, stability, simplicity,

nontoxic elements, and low costs. Graphene and CNTs are promising materials in the development of conductive textiles, ultrathin sensors, and electronic components with their affordability and unique electric and thermal properties (Libertino et al., 2018; Cherenack and Van Pieterson, 2012). The production of smart textiles with sufficient washing performance is promising for the coming future (Ismar et al., 2020; Ruckdashel et al., 2021). Although novel sensors are developed for use in smart clothing, more research is still needed to resolve some technical limitations, such as noise reduction, reliability and security of data transfer, miniaturization, washability, and long-term accuracy in performance, user-friendliness, cost, comfort, health, and safety. Another attractive approach is the fabrication of layered composite textiles. For instance, a textile composed of an outer layer with low thermal conductivity and an inner layer with high thermal conductivity may be promising for cold weather conditions. Moreover, thermal transport can be quenched in textile materials by using aperiodic superlattices in the case of nano-enhanced textile fibers (Chakraborty et al., 2020; Hu et al., 2020b). Fabrication methods such as vacuum-assisted filtration and spraying can be preferred for the production of the high thermally conductive layers, whereas methods such as coating, wet spinning, and chemical coupling may be more suitable for the fabrication of low thermally conductive layers. In the consideration of the data summarized in Figure 10, a single technology such as vacuum-assisted filtration, spraying, and electrospinning can also be adapted to produce composite textile materials with graded conductivity, as the output of these techniques offers a wide range of conductivity.

Besides all these remarkable properties and potential use in a wide range of applications, the smart thermoregulation textiles also possess some challenges. There is still more way in transferring to industrial scale from lab scale. The raw materials should be reachable continuously, and industrial production should be feasible in terms of costs, manufacturing procedures and equipment, ability of design diversity, and dyeability. More effort should be given on research about the air permeability, wearability, biocompatibility, washability, and recyclability of these materials. They should be examined under synergistic parameters, and test methods should be standardized.

ACKNOWLEDGMENTS

O.I.K.-A. acknowledges The Scientific and Technological Research Council of Turkey (TUBITAK)-BIDEB 2218 Project No: 118C485.

REFERENCES

Abbas, A., Zhao, Y., Zhou, J., Wang, X., and Lin, T. (2013). Improving thermal conductivity of cotton fabrics using composite coatings containing graphene, multiwall carbon nanotube or boron nitride fine particles. Fibers Polym. *14*, 1641–1649.

Abu-Thabit, N.Y., and Hamdy Makhlouf, A.S. (2016). Smart textile supercapacitors coated with conducting polymers for energy storage applications. In Industrial Applications for Intelligent Polymers and Coatings, M. Hosseini and A.S. Hamdy Makhlouf, eds. (Springer International Publishing), pp. 437–477.

Akcagun, E., Bogusławska-Baczek, M., and Hes, L. (2019). Thermal insulation and thermal contact properties of wool and wool/PES fabrics in wet state. J. Nat. Fibers *16*, 199–208.

Bhattacharjee, S., Joshi, R., Chughtai, A.A., and Macintyre, C.R. (2019). Graphene modified multifunctional personal protective clothing. Adv. Mater. Inter. *6*, 1900622.

Bhardwaj, N., and Kundu, S.C. (2010). Electrospinning: a fascinating fiber fabrication technique. Biotechnol. Adv. *28*, 325–347.

Bitounis, D., Ali-Boucetta, H., Hong, B.H., Min, D.H., and Kostarelos, K. (2013). Prospects and challenges of graphene in biomedical applications. Adv. Mater. *25*, 2258–2268.

Bonetti, L., Fiorati, A., Serafini, A., Masotti, G., Tana, F., D'Agostino, A., Draghi, L., Altomare, L., Chiesa, R., Farè, S., et al. (2021). Graphene nanoplatelets composite membranes for thermal comfort enhancement in performance textiles. J. Appl. Polym. Sci. *138*, 1–10.

Cheng, M.M., Huang, L.J., Wang, Y.X., Tang, J.G., Wang, Y., Zhao, Y.C., Liu, G.F., Zhang, Y., Kipper, M.J., Belfiore, L.A., et al. (2017). Recent developments in graphene-based/nanometal composite filter membranes. RSC Adv. *7*, 47886–47897.

Canetta, C., Guo, S., and Narayanaswamy, A. (2014). Measuring thermal conductivity of polystyrene nanowires using the dual-cantilever technique. Rev. Sci. Instrum. *85*, 104901.

Chakraborty, P., Liu, Y., Ma, T., Guo, X., Cao, L., Hu, R., and Wang, Y. (2020). Quenching thermal transport in aperiodic superlattices: a molecular dynamics and machine learning study. ACS Appl. Mater. Inter. *12*, 8795–8804.

Chen, H., Ginzburg, V.V., Yang, J., Yang, Y., Liu, W., Huang, Y., Du, L., and Chen, B. (2016). Thermal conductivity of polymer-based composites: fundamentals and applications. Prog. Polym. Sci. *59*, 41–85.

Cherenack, K., and Van Pieterson, L. (2012). Smart textiles: challenges and opportunities. J. Appl. Phys. *112*, 091301.

Chen, Y., Hou, X., Kang, R., Liang, Y., Guo, L., Dai, W., Nishimura, K., Lin, C.T., Jiang, N., and Yu, J. (2018). Highly flexible biodegradable cellulose nanofiber/graphene heat-spreader films with improved mechanical properties and enhanced thermal conductivity. J. Mater. Chem. C *6*, 12739–12745.

Candadai, A.A., Weibel, J.A., and Marconnet, A.M. (2020). Thermal conductivity of ultrahigh molecular weight polyethylene: from fibers to fabrics. ACS Appl. Polym. Mater. *2*, 437–447.

Chen, J., Huang, X., Sun, B., and Jiang, P. (2019). Highly thermally conductive yet electrically insulating polymer/boron nitride nanosheets nanocomposite films for improved thermal management capability. ACS Nano *13*, 337–345.

Chen, L., Xiao, C., Tang, Y., Zhang, X., Zheng, K., and Tian, X. (2019). Preparation and properties of boron nitride nanosheets/cellulose nanofiber shear-oriented films with high thermal conductivity. Ceram. Int. *45*, 12965–12974.

Chen, J., Huang, X., Sun, B., Wang, Y., Zhu, Y., and Jiang, P. (2017). Vertically aligned and interconnected boron nitride nanosheets for advanced flexible nanocomposite thermal

interface materials. ACS Appl. Mater. Inter. *9*, 30909–30917.

Chen, J., Fang, Y., Chen, G., and Bick, M. (2021). Smart textiles for personalized thermoregulation. Chem. Soc. Rev. *50*, 9357.

Chen, J., Wei, H., Bao, H., Jiang, P., and Huang, X. (2019). Millefeuille-inspired thermally conductive polymer nanocomposites with overlapping bn nanosheets for thermal management applications. ACS Appl. Mater. Inter. *11*, 31402–31410.

Cui, S., Jiang, F., Song, N., Shi, L., and Ding, P. (2019). Flexible films for smart thermal management: influence of structure construction of a two-dimensional graphene network on active heat dissipation response behavior. ACS Appl. Mater. Inter. *11*, 30352–30359.

Cui, S., Song, N., Shi, L., and Ding, P. (2020). Enhanced thermal conductivity of bioinspired nanofibrillated cellulose hybrid films based on graphene sheets and nanodiamonds. ACS Sustain. Chem. Eng. *8*, 6363–6370.

Djongyang, N., Tchinda, R., and Njomo, D. (2010). Thermal comfort: a review paper. Renew. Sustain. Energy Rev. *14*, 2626–2640.

Datsyuk, V., Trotsenko, S., Trakakis, G., Boden, A., Vyzas-Asimakopoulos, K., Parthenios, J., Galiotis, C., Reich, S., and Papagelis, K. (2020). Thermal properties enhancement of epoxy resins by incorporating polybenzimidazole nanofibers filled with graphene and carbon nanotubes as reinforcing material. Polym. Test. *82*, 106317.

Dai, M., Zhai, Y., and Zhang, Y. (2021). A green approach to preparing hydrophobic, electrically conductive textiles based on waterborne polyurethane for electromagnetic interference shielding with low reflectivity. Chem. Eng. J. *421*, 127749.

Farajikhah, S., Van Amber, R., Sayyar, S., Shafei, S., Fay, C.D., Beirne, S., Javadi, M., Wang, X., Innis, P.C., Paull, B., et al. (2019). Processable thermally conductive polyurethane composite fibers. Macromol. Mater. Eng. *304*, 1800542.

Fanger, P.O. (1970). Thermal Comfort. Analysis and Applications in Environmental Engineering (Danish Technical Press).

Fu, L., and Yu, A.M. (2014). Carbon nanotubes based thin films: fabrication, characterization and applications. Rev. Adv. Mater. Sci. *36*, 40–61.

Fu, C., Li, Q., Lu, J., Mateti, S., Cai, Q., Zeng, X., Du, G., Sun, R., Chen, Y., Xu, J., et al. (2018). Improving thermal conductivity of polymer composites by reducing interfacial thermal resistance between boron nitride nanotubes. Compos. Sci. Technol. *165*, 322–330.

Gao, J., Hu, M., Dong, Y., and Li, R.K.Y. (2013). Graphite-nanoplatelet-decorated polymer nanofiber with improved thermal, electrical, and mechanical properties. ACS Appl. Mater. Inter. *5*, 7758–7764.

Guo, Y., Yang, X., Ruan, K., Kong, J., Dong, M., Zhang, J., Gu, J., and Guo, Z. (2019). Reduced graphene oxide heterostructured silver nanoparticles significantly enhanced thermal conductivities in hot-pressed electrospun polyimide nanocomposites. ACS Appl. Mater. Inter. *11*, 25465–25473.

Gao, T., Yang, Z., Chen, C., Li, Y., Fu, K., Dai, J., Hitz, E.M., Xie, H., Liu, B., Song, J., et al. (2017). Three-dimensional printed thermal regulation textiles. ACS Nano *11*, 11513–11520.

Guo, R., Ren, Z., Bi, H., Xu, M., and Cai, L. (2019). Electrical and thermal conductivity of polylactic acid (PLA)-based biocomposites by incorporation of nano-graphite fabricated with fused deposition modeling. Polymers (Basel). *11*, 549.

Ghosh, S., Nitin, B., Remanan, S., Bhattacharjee, Y., Ghorai, A., Dey, T., Das, T.K., and Das, N.C. (2020). A Multifunctional smart textile derived from merino wool/nylon polymer nanocomposites as next generation microwave absorber and soft touch sensor. ACS Appl. Mater. Inter. *12*, 17988–18001.

Gspann, T.S., Juckes, S.M., Niven, J.F., Johnson, M.B., Elliott, J.A., White, M.A., and Windle, A.H. (2017). High thermal conductivities of carbon nanotube films and micro-fibres and their dependence on morphology. Carbon N. Y. *114*, 160–168.

Greiner, A., and Wendorff, J.H. (2007). Electrospinning: a fascinating method for the preparation of ultrathin fibers. Angew. Chem. - Int. Ed. *46*, 5670–5703.

Huang, P., Li, Y., Yang, G., Li, Z.X., Li, Y.Q., Hu, N., Fu, S.Y., and Novoselov, K.S. (2021). Graphene film for thermal management: a review. Nano Mater. Sci. *3*, 1–16.

Hu, R., Iwamoto, S., Feng, L., Ju, S., Hu, S., Ohnishi, M., Nagai, N., Hirakawa, K., and Shiomi, J. (2020). Machine-learning-optimized aperiodic superlattice minimizes coherent phonon heat conduction. Phys. Rev. X *10*, 021050.

Hu, R., Xi, W., Liu, Y., Tang, K., Song, J., Luo, X., Wu, J., and Qiu, C.W. (2021). Thermal camouflaging metamaterials. Mater. Today *45*, 120–141.

He, X., and Wang, Y. (2020). Highly thermally conductive polyimide composite films with excellent thermal and electrical insulating properties. Ind. Eng. Chem. Res. *59*, 1925–1933.

Hu, R., Liu, Y., Shin, S., Huang, S., Ren, X., Shu, W., Cheng, J., Tao, G., Xu, W., Chen, R., et al. (2020). Emerging materials and strategies for personal thermal management. Adv. Energy Mater. *10*, 1903921.

Huang, C., Qian, X., and Yang, R. (2018). Thermal conductivity of polymers and polymer nanocomposites. Mater. Sci. Eng. R. Rep. *132*, 1–22.

Han, W., Chen, M., Song, W., Ge, C., and Zhang, X. (2020). Construction of hexagonal boron nitride@polystyrene nanocomposite with high thermal conductivity for thermal management application. Ceram. Int. *46*, 7595–7601.

Ismar, E., Bahadir, S.K., Kalaoglu, F., and Koncar, V. (2020). Futuristic clothes: electronic textiles and wearable technologies. Glob. Challenges *4*, 1900092.

Kim, D., Ha, S., Choi, H.K., Yu, J., and Kim, Y.A. (2018). Chemical assembling of amine functionalized boron nitride nanotubes onto polymeric nanofiber film for improving their thermal conductivity. RSC Adv. *8*, 4426–4433.

Libertino, S., Plutino, M.R., and Rosace, G. (2018). Design and development of wearable sensing nanomaterials for smart textiles. AIP Conf. Proc. *1990*, 020016.

Li, Z., Xu, Z., Liu, Y., Wang, R., and Gao, C. (2016). Multifunctional non-woven fabrics of interfused graphene fibres. Nat. Commun. *7*, 13684.

Liu, Y., and Zhao, X. (2021). The preparation and performance of a polyaniline/graphene composite coated fabric. J. Text. Inst. *112*, 1258–1265.

Lu, C., Chiang, S.W., Du, H., Li, J., Gan, L., Zhang, X., Chu, X., Yao, Y., Li, B., and Kang, F. (2017). Thermal conductivity of electrospinning chain-aligned polyethylene oxide (PEO). Polymer (Guildf). *115*, 52–59.

Li, Y., Porwal, H., Huang, Z., Zhang, H., Bilotti, E., and Peijs, T. (2016). Enhanced thermal and electrical properties of polystyrene-graphene nanofibers via electrospinning. J. Nanomater. *2016*, 4624976.

Ma, J., Zhang, Q., Mayo, A., Ni, Z., Yi, H., Chen, Y., Mu, R., Bellan, L.M., and Li, D. (2015). Thermal conductivity of electrospun polyethylene nanofibers. Nanoscale *7*, 16899–16908.

Maughan, R.J. (2003). Impact of mild dehydration on wellness and on exercise performance. Eur. J. Clin. Nutr. *57*, 19–23.

Majumdar, A., Mukhopadhyay, S., and Yadav, R. (2010). Thermal properties of knitted fabrics made from cotton and regenerated bamboo cellulosic fibres. Int. J. Therm. Sci. *49*, 2042–2048.

Miao, D., Wang, X., Yu, J., and Ding, B. (2021). A biomimetic transpiration textile for highly efficient personal drying and cooling. Adv. Funct. Mater. *31*, 2008705.

Manasoglu, G., Celen, R., Kanik, M., and Ulcay, Y. (2019). Electrical resistivity and thermal conductivity properties of graphene-coated woven fabrics. J. Appl. Polym. Sci. *136*, 48024.

Mittal, G., Rhee, K.Y., Mišković-Stanković, V., and Hui, D. (2018). Reinforcements in multi-scale polymer composites: processing, properties, and applications. Compos. Part B Eng. *138*, 122–139.

Manasoglu, G., Celen, R., Kanik, M., and Ulcay, Y. (2021). An investigation on the thermal and solar properties of graphene-coated polyester fabrics. Coatings *11*, 125.

Nooralian, Z., Parvinzadeh Gashti, M., and Ebrahimi, I. (2016). Fabrication of a multifunctional graphene/polyvinylphosphonic acid/cotton nanocomposite via facile spray layer-by-layer assembly. RSC Adv. *6*, 23288–23299.

Ngo, T.D., Kashani, A., Imbalzano, G., Nguyen, K.T.Q., and Hui, D. (2018). Additive manufacturing (3D printing): a review of materials, methods, applications and challenges. Compos. Part B Eng. *143*, 172–196.

Oğulata, R.T. (2007). The effect of thermal insulation of clothing on human thermal comfort. Fibres Text. East. Eur. *15*, 67–72.

Oner, E. (2019). Mechanical and thermal properties of knitted fabrics produced from various fiber types. Fibers Polym. *20*, 2416–2425.

Park, Y., You, M., Shin, J., Ha, S., Kim, D., Heo, M.H., Nah, J., Kim, Y.A., and Seol, J.H. (2019). Thermal conductivity enhancement in electrospun poly(vinyl alcohol) and poly(vinyl alcohol)/cellulose nanocrystal composite nanofibers. Sci. Rep. *9*, 3026.

Peng, L., Su, B., Yu, A., and Jiang, X. (2019). Review of clothing for thermal management with advanced materials. Cellulose *26*, 6415–6448.

Peng, Y., and Cui, Y. (2020). Advanced textiles for personal thermal management and energy. Joule *4*, 724–742.

Paracha, K.N., Abdul Rahim, S.K., Soh, P.J., and Khalily, M. (2019). Wearable antennas: a review of materials, structures, and innovative features for autonomous communication and sensing. IEEE Access *7*, 56694–56712.

Ruan, K., Guo, Y., Tang, Y., Zhang, Y., Zhang, J., He, M., Kong, J., and Gu, J. (2018). Improved thermal conductivities in polystyrene nanocomposites by incorporating thermal reduced graphene oxide via electrospinning-hot press technique. Compos. Commun. *10*, 68–72.

Ruckdashel, R.R., Venkataraman, D., and Park, J.H. (2021). Smhe future. J. Appl. Phys. *129*, 130903.

Rahman, M.J., and Mieno, T. (2015). Conductive cotton textile from safely functionalized carbon nanotubes. J. Nanomater. *2015*, 978484.

Rahman, N.H.A., Yamada, Y., and Nordin, M.S.A. (2019). Analysis on the effects of the human body on the performance of electro-textile antennas for wearable monitoring and tracking application. Materials (Basel) *12*, 1636.

Song, N., Hou, X., Chen, L., Cui, S., Shi, L., and Ding, P. (2017). A green plastic constructed from cellulose and functionalized graphene with high thermal conductivity. ACS Appl. Mater. Inter. *9*, 17914–17922.

Siddiqui, M.O.R., and Sun, D. (2017). Thermal analysis of conventional and performance plain woven fabrics by finite element method. J. Ind. Textil. *48*, 685–712.

Stevens, K., and Fuller, M. (2015). Thermoregulation and clothing comfort. In Textile-led Design for the Active Ageing Population (Woodhead Publishing), pp. 117–138.

Shu, W., Zhang, X., Yang, X., and Luo, X. (2022). A Smart temperature-regulating garment for portable, high-efficiency and comfortable cooling. J. Electron. Packag. Trans. ASME *144*, 031010.

Song, G., Cao, W., and Cloud, R.M. (2011). Medical textiles and thermal comfort. In Handbook of Medical Textiles, V.T. Bartels, ed. (Woodhead Publishing Limited), pp. 198–218.

Stanković, S.B., Popović, D., and Poparić, G.B. (2008). Thermal properties of textile fabrics made of natural and regenerated cellulose fibers. Polym. Test. *27*, 41–48.

Saji, V.S. (2021). Electrophoretic-deposited superhydrophobic coatings. Chem. - Asian J. *16*, 474–491.

Shim, E. (2019). Coating and laminating processes and techniques for textiles. In Smart Textile Coatings and Laminates, W.C. Smith, ed. (Woodhead Publishing), pp. 11–45.

Soong, Y.-C., and Chiu, C.-W. (2021). Multilayered graphene/boron nitride/thermoplastic polyurethane composite films with high thermal conductivity, stretchability, and washability for adjustable-cooling smart clothes. J. Colloid Interf. Sci. *599*, 611–619.

Song, Y., Jiang, F., Song, N., Shi, L., and Ding, P. (2021). Multilayered structural design of flexible films for smart thermal management. Compos. Part A. Appl. Sci. Manuf. *141*, 106222.

Tang, Z., Yao, D., Du, D., and Ouyang, J. (2020). Highly machine-washable e-textiles with high strain sensitivity and high thermal conduction. J. Mater. Chem. C *8*, 2741–2748.

Tan, C., Dong, Z., Li, Y., Zhao, H., Huang, X., Zhou, Z., Jiang, J.W., Long, Y.Z., Jiang, P., Zhang, T.Y., et al. (2020). A high performance wearable strain sensor with advanced thermal management for motion monitoring. Nat. Commun. *11*, 1–10.

Tabor, J., Chatterjee, K., and Ghosh, T.K. (2020). Smart textile-based personal thermal comfort systems: current status and potential solutions. Adv. Mater. Technol. *5*, 1901155.

Vishnu Chandar, J., Mutharasu, D., Mohamed, K., Marsilla, K.I.K., Shanmugan, S., and Azlan, A.A. (2021). High thermal conductivity, UV-stabilized poly(3-hydroxybutyrate-co-3-hydroxyvalerate) hybrid composites for electronic applications: effect of different hybrid fillers on structural, thermal, optical, and mechanical properties. Polym. Technol. Mater. *60*, 1273–1291.

Wang, F., and Cai, X. (2019). Improvement of mechanical properties and thermal conductivity of carbon fiber laminated composites through depositing graphene nanoplatelets on fibers. J. Mater. Sci. *54*, 3847–3862.

Wang, Z.G., Liu, W., Liu, Y.H., Ren, Y., Li, Y.P., Zhou, L., Xu, J.Z., Lei, J., and Li, Z.M. (2020). Highly thermal conductive, anisotropically heat-transferred, mechanically flexible composite film by assembly of boron nitride nanosheets for thermal management. Compos. Part B Eng. *180*, 107569.

Wu, K., Yu, L., Lei, C., Huang, J., Liu, D., Liu, Y., Xie, Y., Chen, F., and Fu, Q. (2019). Green production of regenerated cellulose/boron nitride nanosheet textiles for static and dynamic personal cooling. ACS Appl. Mater. Inter. *11*, 40685–40693.

Wang, X., Jiang, M., Zhou, Z., Gou, J., and Hui, D. (2017). 3D printing of polymer matrix composites: a review and prospective. Compos. Part B Eng. *110*, 442–458.

Wang, Y., Wang, W., Xu, R., Zhu, M., and Yu, D. (2019). Flexible, durable and thermal conducting thiol-modified rGO-WPU/cotton fabric for robust electromagnetic interference shielding. Chem. Eng. J. *360*, 817–828.

Wei, X., Wang, Z., Tian, Z., and Luo, T. (2021). Thermal transport in polymers: a review. J. Heat Transfer *143*, 072101.

Wang, J., Li, Q., Liu, D., Chen, C., Chen, Z., Hao, J., Li, Y., Zhang, J., Naebe, M., and Lei, W. (2018). High temperature thermally conductive nanocomposite textile by "green" electrospinning. Nanoscale *10*, 16868–16872.

Wang, Z., Mo, L., Zhao, S., Li, J., Zhang, S., and Huang, A. (2018). Mechanically robust nacre-mimetic framework constructed polypyrrole-doped graphene/nanofiber nanocomposites with improved thermal electrical properties. Mater. Des. *155*, 278–287.

Wu, K., Fang, J., Ma, J., Huang, R., Chai, S., Chen, F., and Fu, Q. (2017). Achieving a collapsible, strong, and highly thermally conductive film based on oriented functionalized boron nitride nanosheets and cellulose nanofiber. ACS Appl. Mater. Inter. *9*, 30035–30045.

Wu, K., Liao, P., Du, R., Zhang, Q., Chen, F., and Fu, Q. (2018). Preparation of a thermally conductive biodegradable cellulose nanofiber/hydroxylated boron nitride nanosheet film: the critical role of edge-hydroxylation. J. Mater. Chem. A. *6*, 11863–11873.

Wang, C., Hu, K., Liu, Y., Zhang, M.-R., Wang, Z., and Li, Z. (2021). Flexible supercapacitors based on graphene/boron nitride nanosheets electrodes and PVA/PEI gel electrolytes. Materials (Basel). *14*, 1955.

Xue, Y., Lofland, S., and Hu, X. (2019). Thermal conductivity of protein-based materials: a review. Polymers (Basel). *11*, 456.

Yang, S., Xue, B., Li, Y., Li, X., Xie, L., Qin, S., Xu, K., and Zheng, Q. (2020). Controllable Ag-rGO heterostructure for highly thermal conductivity in layer-by-layer nanocellulose hybrid films. Chem. Eng. J. *383*, 123072.

Yaras, A., Er, E., Celikkan, H., Disli, A., and Alicilar, A. (2016). Cellulosic tent fabric coated with boron nitride nanosheets. J. Ind. Eng. Chem. *45*, 1689–1700.

Yu, X., Li, Y., Wang, X., Si, Y., Yu, J., and Ding, B. (2020). Thermoconductive, moisture-permeable, and superhydrophobic nanofibrous membranes with interpenetrated boron nitride network for personal cooling fabrics. ACS Appl. Mater. Inter. *12*, 32078–32089.

Yang, F., Lan, C., Zhang, H., Guan, J., Zhang, F., Fei, B., and Zhang, J. (2019). Study on graphene/CNC-coated bamboo pulp fabric preparation of fabrics with thermal conductivity. Polymers (Basel) *11*, 1265.

Yu, Q., Weng, P., Han, L., Yin, X., Chen, Z., Hu, X., Wang, L., and Wang, H. (2019). Enhanced thermal conductivity of flexible cotton fabrics coated with reactive MWCNT nanofluid for potential application in thermal conductivity coatings and fire warning. Cellulose *26*, 7523–7535.

Zhao, W., and Hu, R. (2021). Toward high-thermal-conductivity polymers. Matter *4*, 3799–3801.

Zhang, X., Chao, X., Lou, L., Fan, J., Chen, Q., Li, B., Ye, L., and Shou, D. (2021). Personal thermal management by thermally conductive

composites: a review. Compos. Commun. *23*, 100595.

Zhong, Z., Wingert, M.C., Strzalka, J., Wang, H.H., Sun, T., Wang, J., Chen, R., and Jiang, Z. (2014). Structure-induced enhancement of thermal conductivities in electrospun polymer nanofibers. Nanoscale *6*, 8283–8291.

Zhang, Y., Heo, Y.J., Son, Y.R., In, I., An, K.H., Kim, B.J., and Park, S.J. (2019). Recent advanced thermal interfacial materials: a review of conducting mechanisms and parameters of carbon materials. Carbon N. Y. *142*, 445–460.

Zeng, X., Sun, J., Yao, Y., Sun, R., Xu, J.B., and Wong, C.P. (2017). A combination of boron nitride nanotubes and cellulose nanofibers for the preparation of a nanocomposite with high thermal conductivity. ACS Nano *11*, 5167–5178.

Zhang, D.L., Zha, J.W., Li, W.K., Li, C.Q., Wang, S.J., Wen, Y., and Dang, Z.M. (2018). Enhanced thermal conductivity and mechanical property through boron nitride hot string in polyvinylidene fluoride fibers by electrospinning. Compos. Sci. Technol. *156*, 1–7.

Zhao, H., Tian, M., Hao, Y., Qu, L., Zhu, S., and Chen, S. (2018). Fast and facile graphene oxide grafting on hydrophobic polyamide fabric via electrophoretic deposition route. J. Mater. Sci. *53*, 9504–9520.

Zhao, K., Wang, Y., Wang, W., and Yu, D. (2018). Moisture absorption, perspiration and thermal conductive polyester fabric prepared by thiol–ene click chemistry with reduced graphene oxide finishing agent. J. Mater. Sci. *53*, 14262–14273.

Zahid, M., Masood, M.T., Athanassiou, A., and Bayer, I.S. (2018). Sustainable thermal interface materials from recycled cotton textiles and graphene nanoplatelets. Appl. Phys. Lett. *113*, 044103.

Zimniewska, M., Huber, J., Krucińska, I., Torlińska, T., and Kozlowski, R. (2002). The influence of clothes made from natural and synthetic fibres on the activity of the motor units in selected muscles in the forearm - preliminary studies. Fibres Text. East. Eur. *10*, 55–59.

Zou, C., Lao, L., Chen, Q., Fan, J., and Shou, D. (2021). Nature-inspired moisture management fabric for unidirectional liquid transport and surface repellence and resistance. Energy Build *248*, 111203.